Seismic Pressures on Retaining Walls

C Y Chin & Claudia Kayser

Report by:	**Dr C Y Chin** PhD (Cambridge), CEng(UK), EurIng, MICE, FIPENZ Industry Fellow, UC Quake Centre **Dr Claudia Kayser** PhD (Auckland), Dipl.-Ing. (TU-Braunscheweig) Industry Fellow, UC Quake Centre
Reviewed by:	**Professor Michael Pender** PhD (Canterbury), BE (Hons), FIPENZ, Fellow NZSEE University of Auckland
Authorised by:	**Dr Robert Finch** Director, UC Quake Centre

Revision No.	**Description**	**Date**
Draft	Issued for Review	01.08.15
Final	Final copy issued	21.08.15
Final Rev 1	Typographical revisions	09.09.15
Final Rev 2	Revisions	14.03.16

Disclaimer

Executive Summary

This report provides results from carrying out two-dimensional dynamic finite element analyses to determine the applicability of simple pseudo-static analyses for assessing seismic earth forces acting on retaining walls. In particular, this study seeks to determine if the free-field Peak Ground Acceleration (PGA_{ff}) commonly used in these pseudo-static analyses can be optimized. The dynamic finite element analyses considered the following:-

- Embedded cantilever walls with 2m and 3m retained soil heights
- Propped walls with 3m retained soil height and two different prop stiffnesses
- Two soil classes – Class C (Shallow soil) and Class D (Deep soil)
- Three geographical zones:-
    - North Island 1 – Auckland, Hamilton & New Plymouth
    - North Island 2 – Wellington & Palmerston North
    - South Island 1 - Christchurch
- Ensembles of ten acceleration-time histories each for North Island 1 and 2, and six acceleration-time histories for South Island 1
- A total of 946 finite element runs, allowing for magnitude scaling of deconvoluted acceleration amplitudes, for all the above combinations.

Within the parameters assessed, the results of this study revealed the following:-

- Confirmation that simple pseudo-static analyses can provide moderately conservative estimates of seismic earth forces acting on retaining walls based on optimized seismic coefficients.
- Seismic earth forces were found to be sensitive to and dependent on wall displacements, geographical zones and soil classes. A re-classification of wall displacement ranges associated with different geographical zones, soil classes and each of the three pseudo-static methods of calculations (Rigid, Stiff and Flexible wall pseudo-static solutions) is recommended (Table 5-1).
- Use of different ensembles of acceleration-time histories appropriate for the different geographic zones resulted in significantly different calculated seismic earth forces, confirming the importance of using geographic-specific motions.
- For Flexible walls (refer to Table 5-1 for displacement ranges) using the Mononobe-Okabe pseudo-static solution (Okabe, 1926 and Mononobe & Matsuo, 1929), the following percentages of PGA_{ff} can be adopted instead of 100% PGA_{ff}:-
    - North Island 1, Class C: 85%
    - North Island 1, Class D: 100% (no change)

- North Island 2, Class C: 80%
- North Island 2, Class D: 100% (no change)
- South Island 1, Class C: 85%
- South Island 1, Class D: 100% (no change)

- For Stiff walls (based on the Stiff wall pseudo-static solution, Matthewson et al., 1980 and refer to Table 5-1 for displacement ranges), the following percentages of PGA_{ff} can be adopted instead of 100% PGA_{ff} :-
  - North Island 1, Class C: 55%
  - North Island 1, Class D: 100% (no change)
  - North Island 2, Class C: 55%
  - North Island 2, Class D: 100% (no change)
  - South Island 1, Class C: 70%
  - South Island 1, Class D: 100% (no change)
- Walls experiencing very small displacements (refer to Table 5-1 for displacement ranges) resulted in a range of different results:-
  - North Island 1, Class C: 100% PGA_{ff} in Stiff wall solution
  - North Island 1, Class D: 120% PGA_{ff} in Rigid wall solution
  - North Island 2, Class C: 100%PGA_{ff} in Stiff wall solution
  - North Island 2, Class D: 120% PGA_{ff} in Rigid wall solution
  - South Island 1, Class C: 100% PGA_{ff} in Rigid wall solution
  - South Island1, Class D: 120% PGA_{ff} in Rigid wall solution
- The recommended location of the total dynamic active force (comprising both static and dyanamic forces) for all cases is 0.7*H* from the top of the wall (where *H* is the retained soil height).
- Other opportunities to consider for future research include varying wall heights, different types of walls (e.g., tied back and Mechanically Stabilised Earth walls), variations in backfill, retaining walls on slopes and other geographical zones in New Zealand.

Table of Contents

Appendix A – Summary of OpenSees Runs

Appendix B - OpenSees Results

1 Introduction

The determination of seismic earth pressures acting against retaining walls is a complex soil-structure interaction (SSI) problem. Factors which affect these earth pressures include:-

1. The nature of the input motions which includes the amplitude, frequency, directivity and duration of the motion.
2. The response of the soil behind, in front & underlying the wall.
3. The characteristics of the wall, which includes the strength and bending stiffness of the wall.

Due largely to its simplicity, the most common class of analysis for determining the magnitude and distribution of seismic earth pressure acting on a retaining wall is the pseudo-static analysis. This analysis makes use of the free-field Peak Ground Acceleration (PGA_{ff}) typically obtained from national design standards (e.g., NZTA Bridge Manual, 2014). In addition, depending on expected wall displacements under gravity and seismic loading, there are three common solutions associated with this class of analysis. These three solutions are categorised according to increasing retaining wall displacements typically described as Rigid, Stiff or Flexible wall solutions.

Since the early work of Okabe (1926) and Mononobe & Matsuo (1929) in establishing the well-known Mononobe-Okabe (M-O) solution for flexible walls, numerous studies have been carried out to identify whether the full PGA_{ff} as proposed in the M-O solution should be used, or whether a reduction (or increase) to PGA_{ff} can be applied. A similar question can also be asked for the stiff and rigid wall solutions which also incorporate the use of PGA_{ff}.

This study was undertaken in order to provide some evidence to support any reduction (or increase) to PGA_{ff} when using pseudo-static analysis, particularly for New Zealand. In addition, there would also be an opportunity to clarify what displacement ranges might be appropriate for the rigid, stiff and flexible wall solutions.

A non-linear dynamic finite element program, OpenSees, was used to carry out a number of analyses of embedded propped & cantilever retaining walls for shallow & deep soils subject to accelerations appropriate for three geographical areas in the North & South Island of New Zealand. From these analyses, seismic earth forces acting against retaining walls were determined and compared with pseudo-static solutions.

The three main objectives of this study were to:-

1. Compare seismic soil thrusts from OpenSees modelling against pseudo-static analytical methods such as the Rigid, Stiff and Flexible wall solutions & determine if a reduction (or increase) to PGA_{ff}, applied as a seismic coefficient to these solutions, can be justified.
2. Identify the range of wall displacements applicable to the pseudo-static solutions.

3. Determine the location of seismic active soil thrust acting on the retaining wall. This is frequently debated and important particularly for determining the magnitude of bending moment in the retaining wall.

2 Literature Review

2.1 Pseudo-Static Analyses

2.1.1 Rigid Wall Response

Matthewson et al. (1980) and Wood & Elms (1990) both refer to the determination of the dynamic earth pressure for rigid walls as an incremental increase over static earth pressures calculated using the at-rest (K_o) earth pressure coefficient following the solution as proposed in Figure 2-1. This simplified solution is based on elastic solutions developed by Wood (1973). Being a rigid wall response, no wall displacements are assumed.

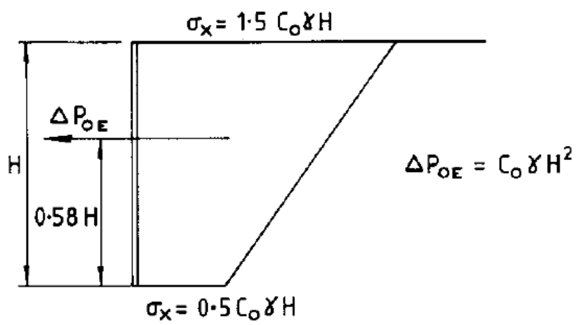

Figure 2-1: Earthquake Induced Pressures on Rigid Wall (Matthewson et al., 1980)

Notes:-

- C_o is Peak Ground Acceleration coefficient referred to as PGA$_{ff}$/g in this study
- ΔP_{OE} is referred to as $\Delta P_{AE,Rigid\ Wall,100\%PGA}$ in this study. The subscript term $_{100\%PGA}$ refers to 100% of PGA$_{ff}$ (refer to further clarification in Section 5)
- *H* is the retained soil height

2.1.2 Stiff Wall Response

Matthewson et al. (1980) describes that for a relatively stiff wall, the earthquake pressures shown in Figure 2-2 should be assumed. They recommend that a movement of the top of the wall of between 0.1%*H* and 0.2%*H* under combined static and dynamic thrusts would be needed to obtain this reduction (i.e., 25% reduction) from the rigid wall pressure. This stiff wall earthquake pressure is an incremental increase over static earth pressures calculated using the active (K_A) earth pressure coefficient.

This method of determining earthquake induced pressures is also cited by Wood & Elms (1990), although they recommend its use for top of wall movements to be between 0%*H* to 0.2%*H*. This is a potential issue as 0%*H* is, in effect, a Rigid wall response.

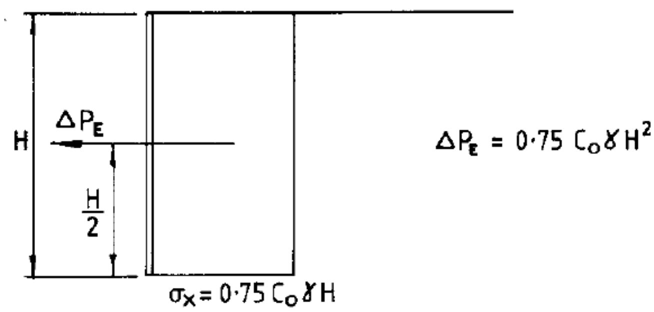

Figure 2-2: Earthquake Induced Pressures on a Deformable (or Stiff) Wall (Matthewson et al., 1980)

Notes:-

- C_o is Peak Ground Acceleration coefficient referred to as PGA_{ff}/g in this study
- ΔP_E is referred to as $\Delta P_{AE,Stiff\ Wall,100\%PGA}$ in this study. The subscript term $_{100\%PGA}$ refers to 100% of PGA_{ff} (refer to clarification in Section 5)

2.1.3 Flexible Wall Response

The flexible wall response typically uses the Mononobe-Okabe (M-O) solution (Okabe, 1926 and Mononobe & Matsuo, 1929), which assumes that sufficient wall movement will need to occur to allow active conditions to develop, provides a convenient method of determining seismic earth pressures acting on retaining walls. This flexible wall earthquake pressure is an incremental increase over static earth pressures calculated using the active (K_A) earth pressure coefficient.

Various publications differ on the magnitude of outward wall deformations (Δh) to allow the use of the M-O solution. These are expressed as ratios of Δh to the exposed wall height (H); $\Delta h/H$. The range of $\Delta h/H$, which the M-O solution is said to apply, varies from $\Delta h/H > 0.1\%$ (Greek Regulatory Guide E39/93) to $\Delta h/H > 0.5\%$ (Matthewson et al., 1980 and Wood & Elms, 1990).

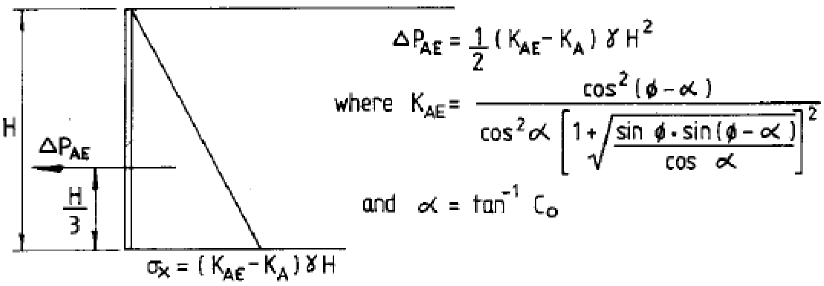

Figure 2-3: Earthquake Induced Pressures on a Flexible Wall (from Matthewson et al., 1980, based on Okabe, 1926 and Mononobe & Matsuo, 1929)

Notes:-

- C_o is Peak Ground Acceleration coefficient referred to as PGA_{ff}/g in this study
- ΔP_{AE} is referred to as $\Delta P_{AE,M-O,100\%PGA}$ in this study. The subscript term *100%PGA* refers to 100% of PGA_{ff} (refer to clarification in Section 5)

2.2 Variations of Seismic Coefficients in Pseudo-Static Analyses

There have been many studies undertaken to establish the validity of the M-O solution. In particular, authors have had differing views on whether the use of PGA_{ff} as the seismic coefficient in the M-O solution results in unconservative, reasonable or conservative solutions.

An unconservative solution would be one where the M-O solution under-predicts the actual dynamic pressure. In comparison, a conservative M-O solution over-predicts the actual dynamic pressure.

An example of a study where the use of PGA_{ff} results in smaller, unconservative values was reported by Green et al. (2003). Seed & Whitman (1970), Whitman (1970) and Steedman & Zeng (1990) reported reasonably matching values of M-O solutions using PGA_{ff}. More recently, reports by Gazetas et al. (2004), Psarropoulos et al. (2005), Anderson et al. (2008) and Atik & Sitar (2010) have suggested that use of PGA_{ff} in M-O solutions can be conservative.

Anderson et al. (2008) described the effects of wave-scattering and proposed height-dependent scaling factors to reduce $PGAs_{ff}$ to be used in M-O solutions for deriving earth pressures. They use US-centric acceleration motions and demonstrate differences in these scaling factors as a function also of location within the United States (Western, Central or Eastern US).

Using centrifuge model testing and numerical analysis of cantilever walls, Atik & Sitar (2010) propose amongst other recommendations that for both stiff and flexible walls, using 65% of the PGA with the M-O method provides a good agreement with measured and calculated pressures.

As the seismic events used by the above authors have unique seismic signatures which may not apply to New Zealand, the basis of this study was to carry out two-dimensional dynamic numerical analyses based on acceleration records which would be applicable to New Zealand (Section 4.2).

3 OpenSees

Two-dimensional finite element (FE) analyses were performed for this project using the Open System for Earthquake Engineering Simulation (OpenSees), which is an object-oriented open source software framework developed by the Pacific Earthquake Engineering Research (PEER) Centre. OpenSees allows users to simulate the responses of structural and geotechnical systems subjected to earthquakes (http://opensees.berkeley.edu).

OpenSees contains a large library of both linear and non-linear geotechnical and structural materials to enable realistic simulations. Details of modelling used in this study are described below (Sections 3.1 to 3.4).

The software GiD (http://www.gidhome.com) was used as a pre-processor to develop Tcl scripts for OpenSees to create model meshes and, soil and structural nodes & elements. An example of a GiD model, at various construction stages (as modelled in OpenSees) is presented in Figure 3-1. Results obtained from OpenSees were post-processed using Matlab (http://www.mathworks.com).

3.1 OpenSees Models

Six base models were created within OpenSees. These represented the following soil classes and wall types (Table 3-1). An example of a Class C propped wall and a Class D embedded cantilever wall is given in Figure 3-2 and Figure 3-3 respectively. Details of runs will be discussed in Section 4:-

Table 3-1: Base Model Details

Soil Class	**Soil Profile/Period**	**Wall Type**
Class C – Shallow soils	10m Medium dense Sand overlying Bedrock. Retained soil comprises Medium dense Gravel Calculated period 0.28 secs.	Embedded cantilever; 2m retained soil height; 5m overall wall height.
		Embedded cantilever; 3m retained soil height; 8m overall wall height.
		Two-level propped wall; 3m retained soil height; 8m overall wall height. Props located at top of wall and 2.5m from top of wall.
Class D – Deep soils	6m Medium dense Sand overlying 10m Loose Sand overlying Bedrock. Retained soil comprises Medium dense Gravel Calculated period of 0.84 secs.	Embedded cantilever; 2m retained soil height; 5m overall wall height.
		Embedded cantilever; 3m retained soil height; 8m overall wall height.
		Two-level propped wall; 3m retained soil height; 8m overall wall height. Props located at top of wall and 2.5m from top of wall.

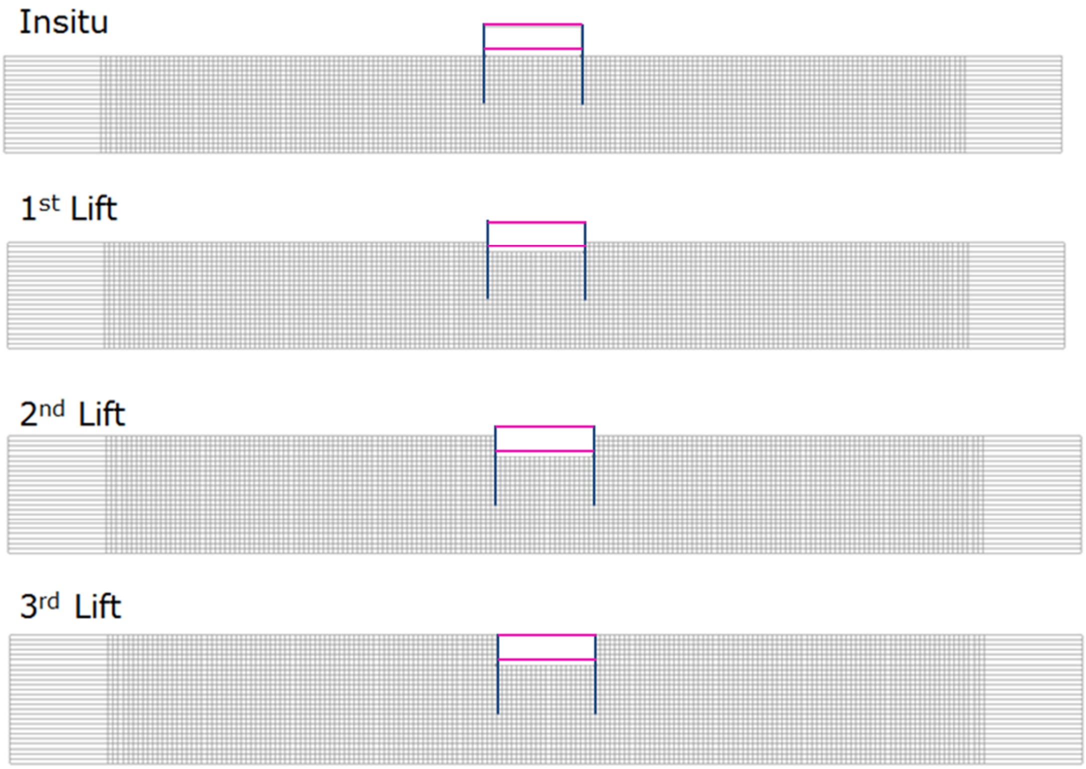

Figure 3-1: Class C Propped Wall Staged Construction

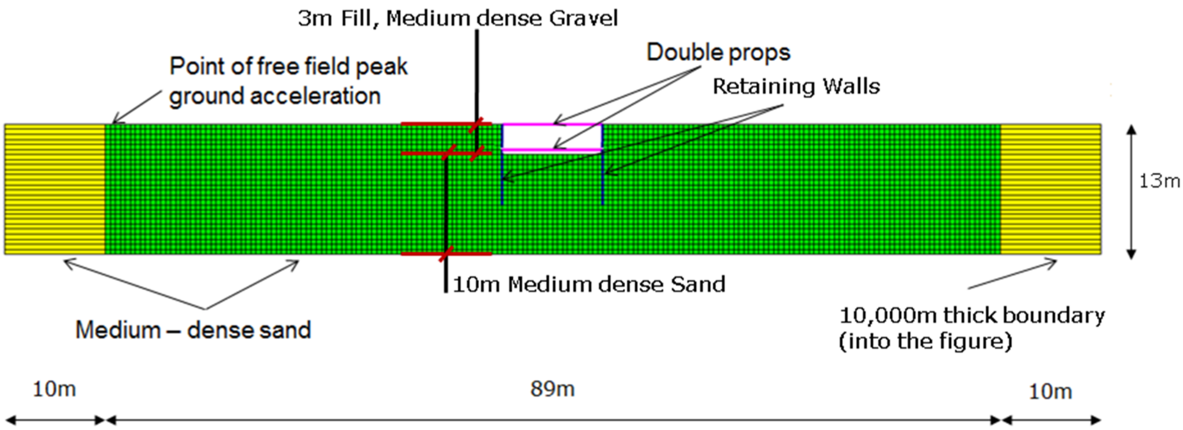

Figure 3-2: Example of Class C Propped Wall OpenSees Model

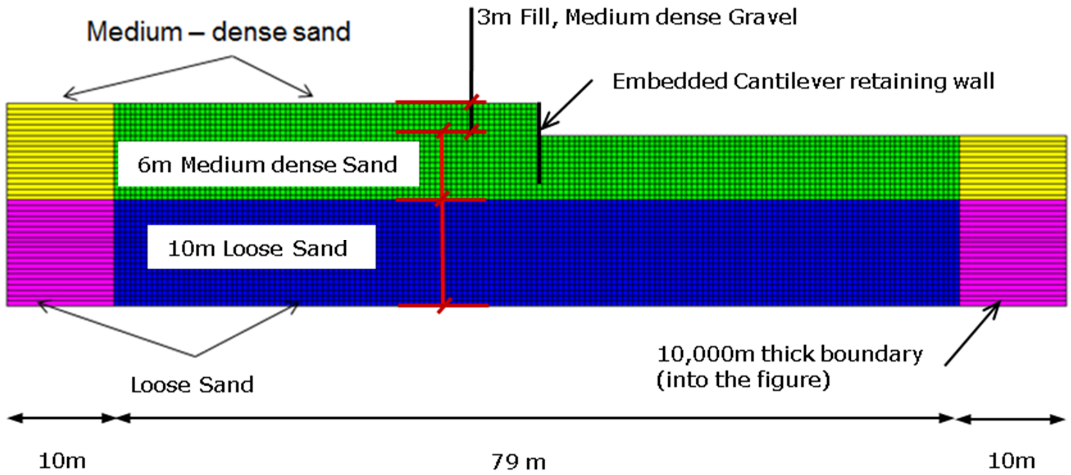

Figure 3-3: Example of Class D Embedded Cantilever Wall

The selection of soil element size in the OpenSees model was based on the recommendation of Kuhlemeyer & Lysmer (1973) and Smith (1975) that the element length in the direction of propagation should be less than one-eighth of the shortest wave length. An initial approximation of an appropriate maximum element length was based on a maximum shear wave frequency of 15Hz (e.g., Zhang et al., 2008) and an average shear wave velocity of ~140m/s. This suggested a maximum element length of 1m. The final soil element length adopted for all analyses was 0.5m. Subsequent assessments of mean periods for all runs based on Rathje (2004) confirmed the appropriateness of an element length of 0.5m. Damping to all elements and nodes was set at 5%.

3.2 OpenSees Materials

Soil properties were modelled using the PressureDependMultiYield02 (PDMY02) material from OpenSees, which is an elastic-plastic material specially created to simulate a non-linear stress-strain relationship under general loading conditions. Such characteristics include dilatancy (shear-induced volume contraction or dilation) and non-flow liquefaction (cyclic mobility), typically exhibited in sands or silts during monotonic or cyclic loading. Under gravity (static) loading, the material behaviour is linear elastic. In subsequent dynamic loading phases, the stress-strain response is elastic-plastic. Plasticity is formulated based on the multi-surface (nested surfaces, see Figure 3-4) concept, with a non-associative flow rule to reproduce the dilatancy effect. All soils were modelled as dry.

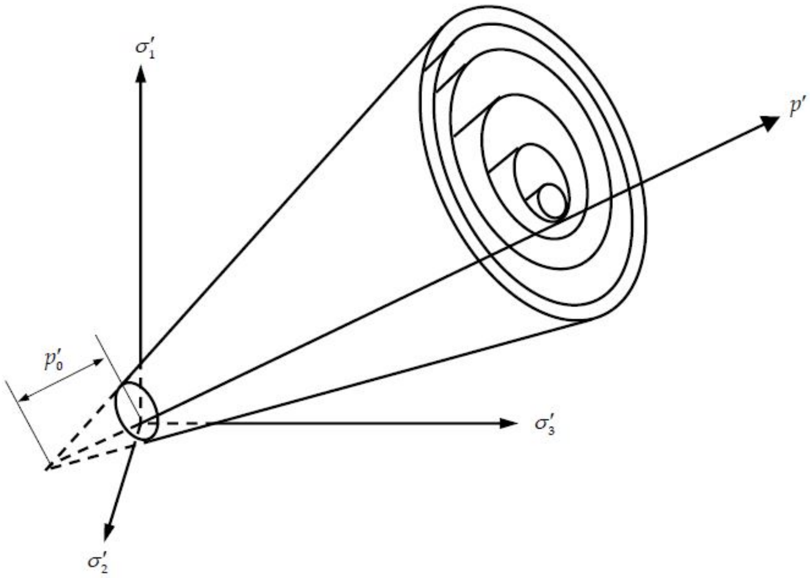

Figure 3-4 Conical Nested Yield Surfaces in Principal Stress Space (after Parra-Colmenares, 1996)

An overview of the adopted soil properties is given in Table 3-2 below.

Table 3-2: PDMY02 Properties

OpenSees input	Variable	Medium dense Sand/Gravel	Loose Sand	Description
rho_soil_1	ρ	2.0	1.8	Soil mass density (t/m^3)
G1	G_r	41298	67514	Reference low-strain shear modulus, specified at a reference mean effective confining pressure refPress_1 (kPa)
B1	K_r	123893	180263	Reference bulk modulus, specified at a reference mean effective confining pressure refPress_1 (kPa)

frictionAng_1	φ	36.5	32.0	Friction angle at peak shear strength (°), which is the same as the friction angle in a triaxial test
peakShearStra_1	$\gamma_{max,r}$	0.1	0.1	An octahedral shear strain at which the maximum shear strength is reached, specified at a reference mean effective confining pressure refPress_1
refPress_1	p'_r	101.0	101.0	Reference mean effective confining pressure (kPa)
pressDependCoe_1	d	0.5	0.5	A positive constant defining variations of G and B as a function of instantaneous effective confinement
PTAng_1	φ_{PTAng}	26.0	27.0	Phase transformation angle (°)
contrac1_1	c_1	0.013	0.013	A non-negative constant defining the rate of shear-induced volume decrease (contraction) or pore pressure build up. A larger value corresponds to faster contraction rate
contrac2_1	c_2	5.0	5.0	
contrac3_1	c_3	0.0	0.0	
dilat1_1	d_1	0.3	0.3	Non-negative constant defining the rate of shear-induced volume increase (dilation). Larger values correspond to stronger dilation rate.

dilat2_1	d_2	3.0	3.0	
dilat3_1	d_3	0.0	0.0	
liquefac1_1	liq_1	1.0	1.0	Parameters controlling the mechanism of liquefaction-induced perfectly plastic shear strain accumulation, i.e., cyclic mobility.
liquefac2_1	liq_2	0.0	0.0	
noyield_1	*NYS*	20	20	Number of yield surfaces
void_1	*e*	0.55	0.71	Initial void ratio
cs1 cs2 cs3	cs_1 cs_2 cs_3	0.9 0.02 0.7	0.9 0.02 0.7	
nDMaterial PressureDependMultiYield02 1 2 $rho_soil_1 $G1 $B1 $frictionAng_1 $peakShearStra_1 $refPress_1 $pressDependCoe_1 $PTAng_1 $contrac1_1 $contrac3_1 dilat1_1 $dilat3_1 $noyield_1 $contrac2_1 $dilat2_1 $liquefac1_1 $liquefac2_1 $void_1 $cs1 $cs2 $cs3 101.0;				

3.3 OpenSees Elements

The two-dimensional OpenSees model adopted the following element set-ups:

- All soil elements have two degrees of freedom (2DOF) and all wall elements have three degrees of freedom (3DOF).
- Soil elements comprise SSPQuad elements. The SSPQuad element is a four-node quadrilateral element using physically stabilised single-point integration with a single Gauss integration point in the centre of each element. SSP stands for “Stabilised Single Point” and this stabilisation incorporates an assumed strain field in which the volumetric dilation and the shear strain associated with the hourglass modes are zero (McGann et al., 2012).

- The wall was modelled using ElasticBeamColumn Elements. The 2-dimensional OpenSees analysis requires properties on a per-metre (into the page) basis which were calculated from 750mm diameter reinforced concrete piles at 2.25m spacing with the following properties:-
    - Concrete compressive strength f_s = 35MPa
    - E = 27.806GPa
    - A = 0.19634954 m^2/m
    - I = 0.00690291m^4/m
    - Mass m = 0.49t/m-length/m-spacing
- Where a propped wall was modelled, two levels of props were used. The pair of props was modelled as massless, elastic members with the same stiffness properties. Sensitivity runs were carried out with two pairs of props, each with different stiffnesses. These were:-

    1. Type “2P” Prop (Refer to Appendix A – Summary of OpenSees Runs, Nomenclature Fff)

        E = 30.38GPa

        A = 0.4m^2/m

        I = 0.0154m^4/m

    2. Type “2Pa” Prop (Refer to Appendix A – Summary of OpenSees Runs, Nomenclature Fff)

        E = 30.38GPa

        A = 0.0004m^2/m

        I = 0.0000154m^4/m

- Connections between soil and wall were established with ZeroLength Elements (ZLE) and Equal Degrees of Freedom (EqualDOFs). The ZLEs represent the interface between soil and wall and the EqualDOFs allows the connection between 2DOF (soil) and 3DOF (wall) elements.

- Two materials were chosen to model the soil-wall interface. In the x-direction, a uniaxial Elastic-No Tension (ENT) material was chosen and in y-direction an Elastic-Perfectly Plastic (ElasticPP) material. The uniaxial ENT material allows soil to act in compression against the wall and to allow separation to occur when soil moves away from the wall. The uniaxial ENT material varied with depth and was based on the Young's Modulus of the surrounding soil. The ElasticPP material was modelled with a Young's modulus of 3900 kPa. The representative strain varied with every 0.5m of depth and was chosen based on a maximum allowable ratio of soil-wall friction (δ/ϕ') of 0.5.

3.3.1 ZeroLength Element

The ZLE was used to model the reaction (force-deformation relationship) between the soil and the wall and is defined by two uniaxial materials that provide the direction of the element (see https://searchcode.com/codesearch/view/13042539/). The ENT material acts in the x-direction and the ElasticPP in the y-direction as mentioned above. To connect the ZLE between soil and wall, a dummy node was introduced to establish an equal DOF connection (in both x- and y-direction) between wall and dummy (3DOF to 2DOF) nodes. See Figure 3-5 below for further clarification. This allowed for the construction of the element in a domain of 2 dimensions with 2 DOFs. The two nodes (i and j) which make up the element are at the same coordinates, hence the term "ZeroLength".

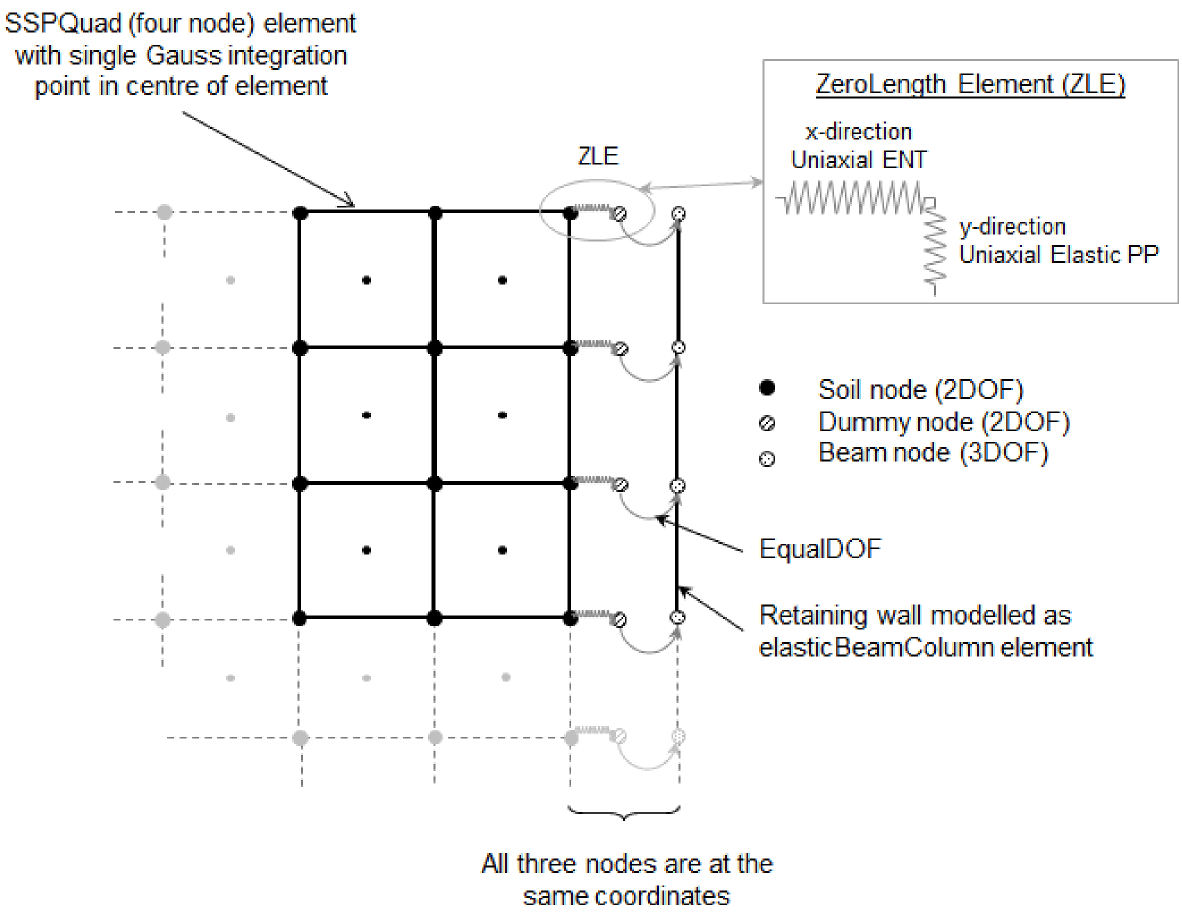

Figure 3-5 Configuration of Soil and Wall Interaction

The above soil-wall interface modelling was based on Atik and Sitar (2008) who reported comparable results between centrifuge model testing and OpenSees modelling. The use of ZLE with ENT was found to be stable in this study.

3.4 OpenSees Boundary Conditions

Boundary conditions were chosen based on McGann & Arduino (2015). Free-field boundary conditions were modelled using 10m wide and 10,000m thick (into the page) columns (See Figure 3-2 and Figure 3-3).

In static conditions the base was fixed in x- and y-directions. For dynamic analysis, the boundary conditions at the base were changed to allow fixity in the y-direction only, as shown in Figure 3-6. The earthquake motion is applied in x-direction at node number 1, which is the overall master node. Node 1 was connected with equal DOF (in x-direction only) to all base nodes (1 to 2, 1 to 3, 1 to 4, etc.) as well as to the dashpot node. This ensures that the earthquake motion is applied along the entire base of the model. The input file for OpenSees was given as a velocity-time history and was obtained by integrating the respective deconvoluted acceleration-time history file. Deconvolution is discussed in Section 4.3.

Within each free-field boundary column, nodes were connected horizontally via EqualDOFs as shown in Figure 3-6 below.

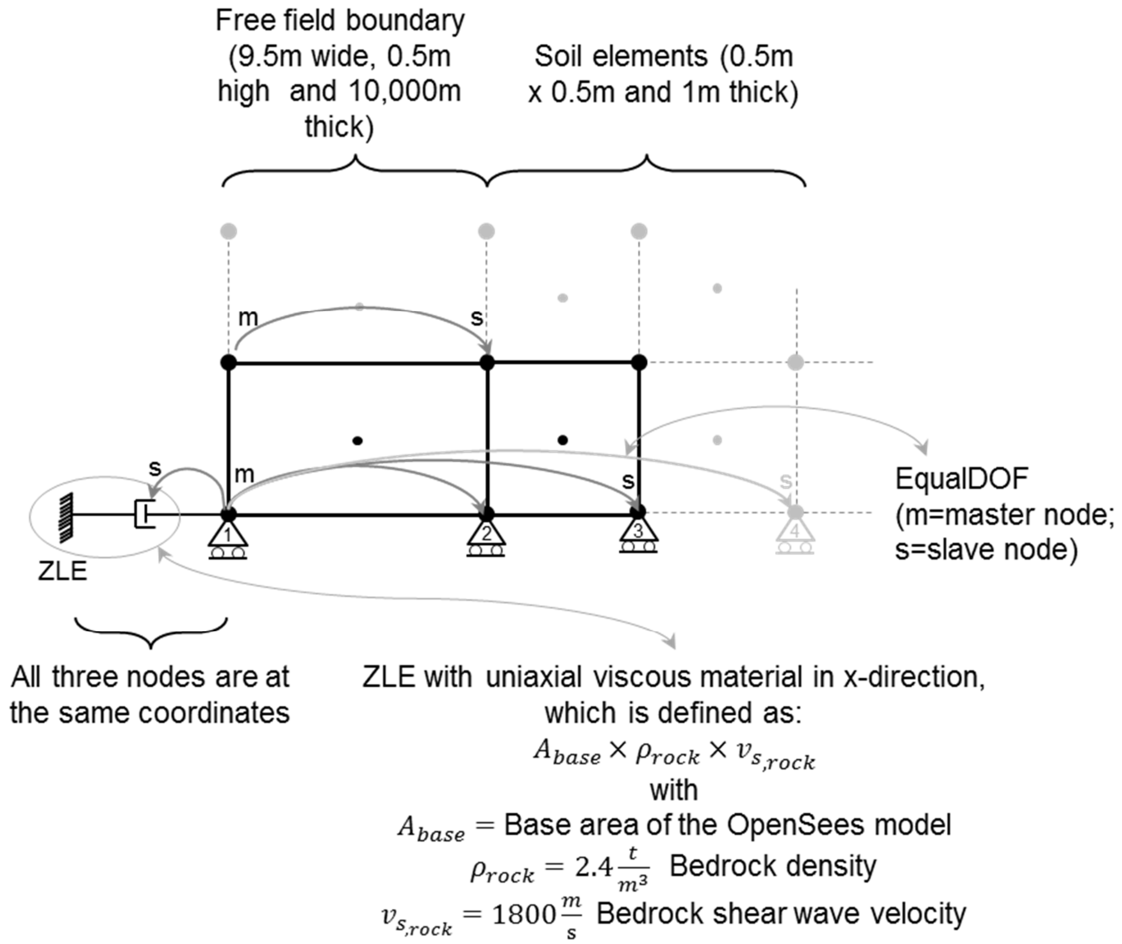

Figure 3-6 Boundary Conditions at Base of Model during Dynamic Analysis

4 Analyses

OpenSees provides a number of algorithms to solve the system of equations. The Krylov Newton algorithm was selected, which was found to be generally faster than other Newtonian algorithms and more stable compared to other methods (Scott & Fenves, 2010).

4.1 Runs

The following combinations of dynamic FE analyses were undertaken in OpenSees. A summary of all runs is presented in Appendix A:-

• 2 soil classes (Classes C & D)	2
• Acceleration-time histories	
o North Island 1 & 2	10
o South Island (Christchurch)	6
• Approximately 7 amplitude scalings per time history	~7
• 2 embedded cantilever wall heights	2
• 1 double propped wall with 2 variations of prop stiffness	2
• 1 type of backfill	1
Total number of runs	946

4.2 Selection of Ground Motions

Various characteristics of seismic motions (including PGA, frequency content, directivity and duration) are known to influence the response of soil, and consequently the dynamic soil pressures acting against the retaining wall. For this study, soil classes were obtained from NZS 1170.5:2004. The two most common classes of soil, Classes C and D, were modelled. Representative soil profiles are described in Table 3-1.

Representative ground motions were selected for three geographical zones as follows:-

1. North Island 1 (NI1) (ref: Zone North A (Oyarzo-Vera et al., 2012)) which includes Auckland, Hamilton & New Plymouth.
2. North Island 2 (NI2) (ref: Zone North NF (Oyarzo-Vera et al., 2012)) which includes Wellington & Palmerston North.
3. South Island 1 (SI1) (ref: Tarbali & Bradley, 2014) which covers Christchurch.

For the North Island, Oyarzo-Vera et al. (2012) conducted deaggregations of a probabilistic seismic hazard model and the seismological characteristics of expected ground motions at different locations of the North Island (Figure 4-1). For this study, acceleration-time histories from two zones (Zone North A and Zone North NF) were used.

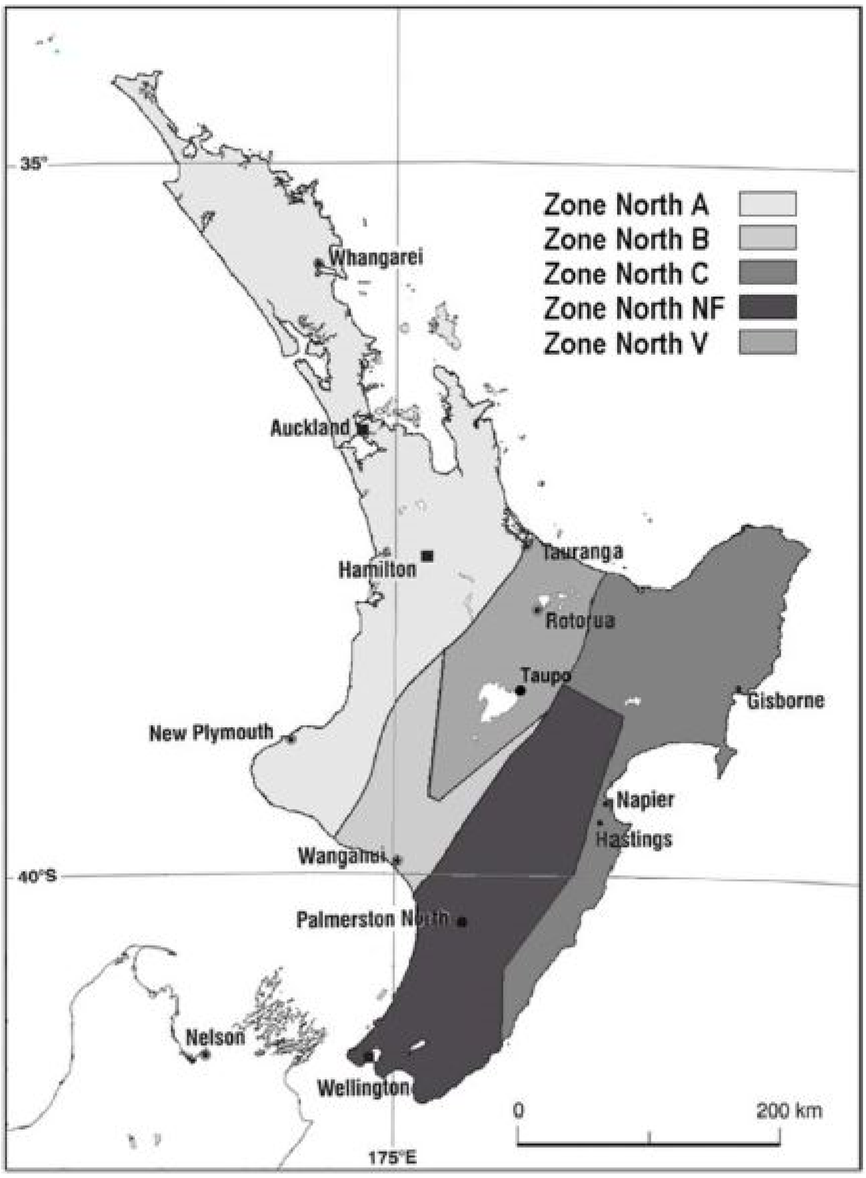

Figure 4-1 Geographical Zonation for North Island (Ref: Oyarzo-Vera et al., 2012)

For Christchurch, ground motions recommended by Tarbali & Bradley (2014) using the Generalized Conditional Intensity Measure (GCIM) approach were used. Tarbali and Bradley (2014) recommended ensembles of seven ground motions for each of the Alpine, Hope and Porters Pass earthquakes. For this study, a total of six ground motions (two motions from each earthquake) were selected.

Depending on the appropriate soil class (Class C or D, refer to Table 3-1), appropriate motions for NI1, NI2 and SI1 are as follows (Table 4-1, Table 4-2 & Table 4-3).

Table 4-1 North Island 1 (NI1) Ground Motions

Event	Year	M_w*	Mechanism	PGA(g)
Class C - Shallow soils				
El Centro, Imperial Valley, USA	1940	7.0	Strike-Slip	0.21
Delta, Imperial Valley, USA	1979	6.5	Strike-Slip	0.34
Bovino, Campano Lucano, Italy	1980	6.9	Normal	0.05
Kalamata, Greece	1986	6.2	Normal	0.23
Matahina Dam D, Edgecumbe, NZ	1999	6.2	Strike-slip	0.28
Class D - Deep soils				
El Centro, Imperial Valley, USA	1940	7.0	Strike-Slip	0.21
Delta, Imperial Valley, USA	1979	6.5	Strike-Slip	0.34
Kalamata, Greece	1986	6.2	Normal	0.23
Corinthos, Greece	1981	6.6	Normal	0.31
Westmorland, Superstition Hill, USA	1987	6.5	Strike-Slip	0.21

Note: M_w* - Moment magnitude

Table 4-2 North Island 2 (NI2) Ground Motions

Event	Year	M_w*	Mechanism	PGA(g)
Class C - Shallow soils				
Duzce, Turkey	1999	7.1	Oblique	0.50
Arcelik, Kocaeli, Turkey	1999	7.5	Strike-Slip	0.21
La Union, Mexico	1985	8.1	Subduction interface	0.16
Lucerne, Landers, USA	1992	7.3	Strike-Slip	0.60
Tabas, Iran	1978	7.4	Reverse	0.93
Class D - Deep soils				
El Centro, Imperial Valley, USA	1940	7.0	Strike-Slip	0.21
Duzce, Turkey	1999	7.1	Oblique	0.50
El Centro #6, Imperial Valley, USA	1979	6.5	Reverse	0.44
Caleta de Campos, Mexico	1985	8.1	Subduction interface	0.14
Yarimka YPT, Kocaeli, Turkey	1999	7.5	Strike-Slip	0.22

Note: M_w* - Moment magnitude

Table 4-3 South Island 1 (SI1) Ground Motions, Classes C & D

Record Sequence Number	Event	Year	Station	M_w*	Mechanism	PGA(g)
Alpine fault scenario rupture						
888	Landers	1992	San Bernardino - E & Hospitality	7.28	Strike-Slip	0.08
1188	Chi-Chi, Taiwan	1999	CHY016	7.62	Reverse-Oblique	0.10
Hope fault scenario						
1147	Kocaeli, Turkey	1999	Ambarli	7.51	Strike-Slip	0.21
1766	Hector Mine	1999	Baker Fire Station	7.13	Strike-Slip	0.11
Porters Pass fault scenario						
93	San Fernando	1971	Whittier Narrows Dam	6.61	Reverse	0.12
1026	Northridge-01	1994	Lawndale - Osage Ave	6.69	Reverse	0.12

Note: M_w* - Moment magnitude

4.3 Deconvolution of Acceleration-Time Records

The acceleration-time histories from Section 4.2 are ground motions. As the OpenSees model requires velocity-time histories to be input at the base of the model, ground acceleration-time histories were first deconvoluted (e.g., Mejia & Dawson, 2006). This was carried out using STRATA (2013) based on one-dimensional (1D) equivalent linear analyses. The deconvoluted acceleration signals at the base of the 1D column were subsequently integrated to provide velocity-time histories that were applied at the base of the OpenSees model.

In order to determine the reasonableness of acceleration-time histories at ground level which were propagated up from the base of the model, sample comparisons of the ground acceleration-spectra, frequency content (with Fast Fourier Transform analyses) and acceleration-time histories were carried out between the original acceleration-time histories and free-field acceleration-time histories from the OpenSees model. These showed reasonable matches, in spite of different assumptions made in carrying out deconvolution (based on equivalent linear analyses with G/G_{max} variations per meter depth) and the subsequent propagation of deconvoluted signals (based on non-linear assumptions made in OpenSees).

5 Results

The aims of the analyses undertaken were as follows:-

- Determine the dynamic active force (ΔP_{AE}) defined as the incremental force exceeding the static force, acting over the retained soil height on the active side of the retaining wall during a seismic event. Four methods of determining ΔP_{AE} were used – these were with (1) OpenSees, (2) Rigid wall (Matthewson et al., 1980), (3) Stiff wall (Matthewson et al., 1980) and (4) Mononobe-Okabe (M-O) methods. The intention was to compare the maximum ΔP_{AE} obtained from OpenSees with the other three pseudo-static methods based on PGA_{ff} obtained from OpenSees runs. These comparisons were assessed against wall displacements predicted in OpenSees.

    - Where ΔP_{AE} was calculated using results from OpenSees, this was denoted by the term $\Delta P_{AE,OpenSees}$. Forces in the Elastic No-Tension Zero-Length elements (ENT-ZLEs) which connect the soil to the wall were integrated over the retained soil height for each time step of the dynamic analysis. $\Delta P_{AE,OpenSees}$ was determined at each time step by subtracting the integrated force measured in the ENT-ZLEs at the end of static loading from those recorded during the seismic shaking. For a given dynamic run, the maximum $\Delta P_{AE,OpenSees}$ was used to compare against ΔP_{AE} calculated using other pseudo-static methods below.

    - Calculate ΔP_{AE} using the rigid wall equation recommended by Matthewson et al. (1980) and Wood & Elms (1990).

      $$\Delta P_{AE,Rigid\ Wall,X\%PGA} = C(0).\gamma.H^2$$

      The seismic coefficient, $C(0)$, is referred to as a fraction of PGA_{ff}/g based on the percentage of PGA_{ff} denoted by the subscript $_{X\%PGA}$, where X is the percentage of PGA_{ff}. Hence, $\Delta P_{AE,Rigid\ Wall,80\ \%PGA}$ indicates that 80% of PGA_{ff} expressed as a fraction of g was assumed to be the seismic coefficient. In this report, the convention of ΔP_{AE} has been used instead of ΔP_{OE} found in Matthewson et al. (1980).

    - Calculate ΔP_{AE} using the stiff wall equation recommended by Matthewson et al. (1980) and Wood & Elms (1990).

      $$\Delta P_{AE,Stiff\ Wall,X\%PGA} = 0.75\ C(0).\gamma.H^2$$

      The seismic coefficient, $C(0)$, is referred to as a fraction of PGA_{ff}/g based on the percentage of PGA_{ff} denoted by the subscript $_{X\ \%PGA}$, where X is the percentage of PGA_{ff}. Hence, $\Delta P_{AE,Stiff\ Wall,80\ \%PGA}$ indicates that 80% of PGA_{ff} expressed as a fraction of g was assumed to be the seismic coefficient. In this report, the convention of ΔP_{AE} has been used instead of ΔP_{E} found in Matthewson et al. (1980).

- Calculate ΔP_{AE} for flexible walls using the Mononobe-Okabe (M-O) method:

$$\Delta P_{AE,M-O,X\%PGA} = \frac{1}{2}(K_{AE} - K_A).\gamma.H^2$$

  The seismic coefficient assumed in the M-O calculation is referred to as a fraction of PGA_{ff}/g based on the percentage of PGA_{ff} denoted by the subscript $_{X\,\%PGA}$, where X is the percentage of PGA_{ff}. Hence, $\Delta P_{AE,M\text{-}O,80\,\%PGA}$ indicates that 80% of PGA_{ff} expressed as a fraction of g was assumed to be the seismic coefficient. Wall friction was assumed to be 0.5 to coincide with assumptions made in OpenSees.

- Determine the average wall displacement (Δh_{avg}) due to both static and dynamic loads over the retained height of the retaining wall in the OpenSees analyses.

  Where Δh_{avg} = Average of ($\Delta h_{t,max}$ - $\Delta h_{ff,t,max}$) over the exposed wall height

  $\Delta h_{t,max}$ is the maximum absolute displacement profile of the wall at a given time during the seismic event. This profile may not coincide with the time of maximum $\Delta P_{AE,OpenSees}$

  $\Delta h_{ff,t,max}$ is the free-field soil displacement profile at the time of $\Delta h_{t,max}$

- Determine the Arias intensity as defined by Arias (1970) as:-

$$I_{xx} = \frac{\pi}{2g}\int_0^\infty a_x(t)^2\,dt$$

  Where I_{xx} is the Arias Intensity in units of length per time along the x-axis

  $a_x(t)$ is the acceleration-time history in units of g along the x-axis

  g is the acceleration of gravity

Results of the 946 OpenSees runs were collated and for each run, a PGA_{ff} was established. These PGA_{ff}'s were used to calculate $\Delta P_{AE,Rigid\ Wall}$, $\Delta P_{AE,Stiff\ Wall}$ and $\Delta P_{AE,M\text{-}O}$ and comparisons against $\Delta P_{AE,OpenSees}$ were made. These are reported below (Sections 5.1 to 5.3) according to the various geographical zones and soil classes.

In making comparisons of the dynamic active forces between $\Delta P_{AE,OpenSees}$ and those from pseudo-static analyses, a fraction of PGA_{ff} would be used in the pseudo-static analysis to either match or over-estimate dynamic active forces calculated using OpenSees. This was done to maintain a moderately conservative approach for design using these pseudo-static solutions.

5.1 North Island 1 – Auckland, Hamilton & New Plymouth

5.1.1 NI1 Soil Class C

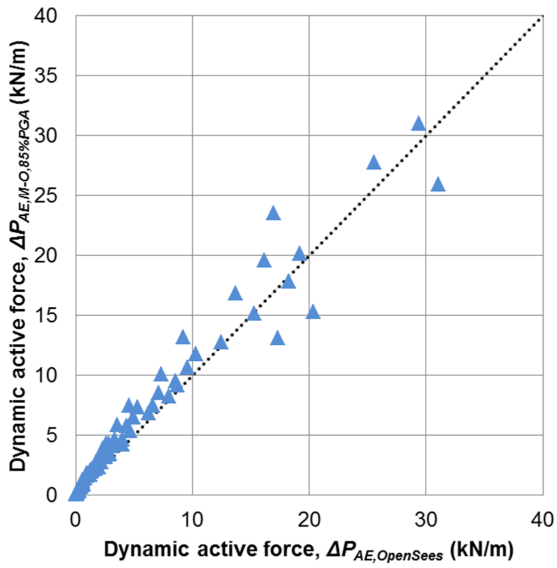

Figure 5-1 Comparison of Dynamic Active Forces $\Delta P_{AE\ OpenSees}$ vs $\Delta P_{AE,M\text{-}O,85\%PGA}$ for NI1 Soil Class C, $(\Delta h_{avg}/H) \geq 0.2\%$ and $PGA_{ff} < 0.7g$

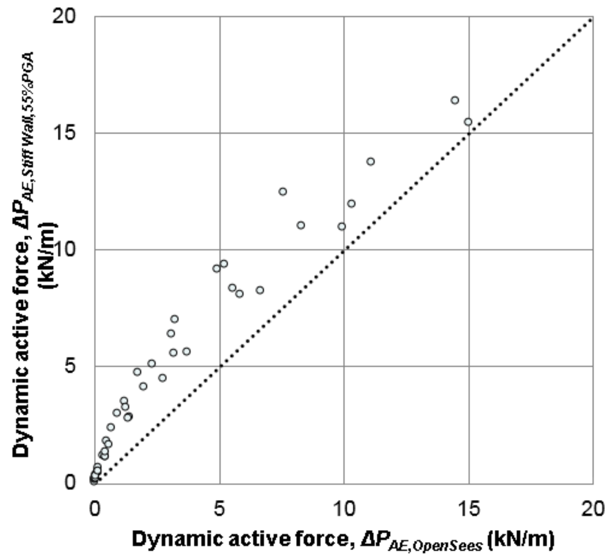

Figure 5-2 Comparison of Dynamic Active Forces $\Delta P_{AE\ OpenSees}$ vs $\Delta P_{AE,Stiff\ Wall,55\%PGA}$ for NI1 Soil Class C, $0.1\% \leq (\Delta h_{avg}/H) < 0.2\%$ and $PGA_{ff} < 0.23g$

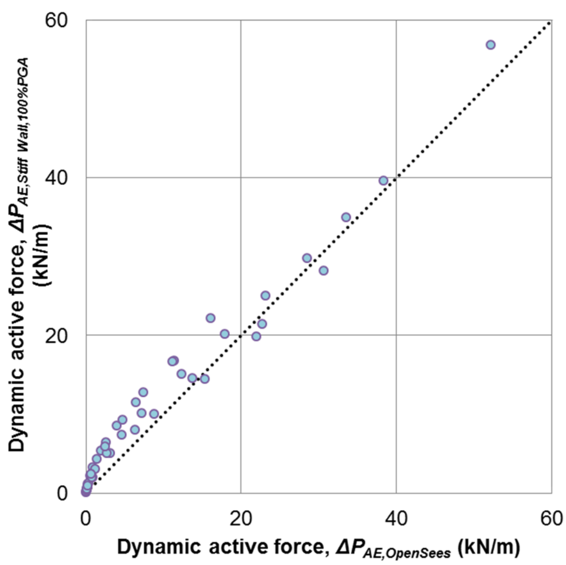

Figure 5-3 Comparison of Dynamic Active Forces $\Delta P_{AE\ OpenSees}$ vs $\Delta P_{AE,Stiff\ Wall,100\%PGA}$ for NI1 Soil Class C, $(\Delta h_{avg}/H) < 0.1\%$ and $PGA_{ff} < 0.43g$

Summary of findings for Dynamic active force $\Delta P_{AE\ OpenSees}$: NI1 Soil Class C			
Normalised average wall displacements due to both static and dynamic loads $(\Delta h_{avg}/H)$ %	**Recommended Seismic coefficient ($\%PGA_{ff}$) used in pseudo-static calculations**		
	Flexible (M-O)	**Stiff**	**Rigid**
< 0.1%	-	100%	-
≥ 0.1% and < 0.2%	-	55%	-
≥ 0.2%	85%	-	-

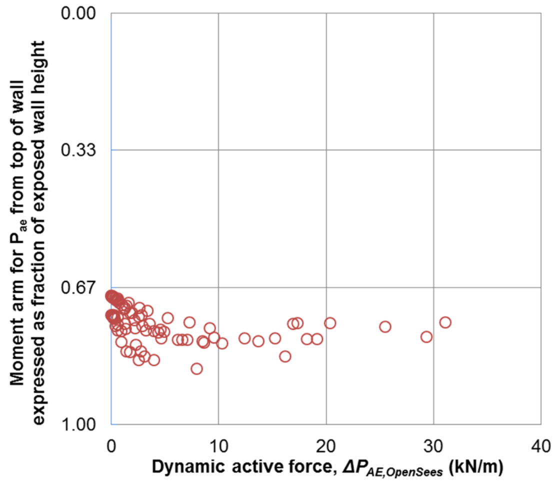

Figure 5-4 Resultant Location of $P_{ae,OpenSees}$ for NI1 Soil Class C, ($\Delta h_{avg}/H$) ≥ 0.2% and PGA$_{ff}$ < 0.7g

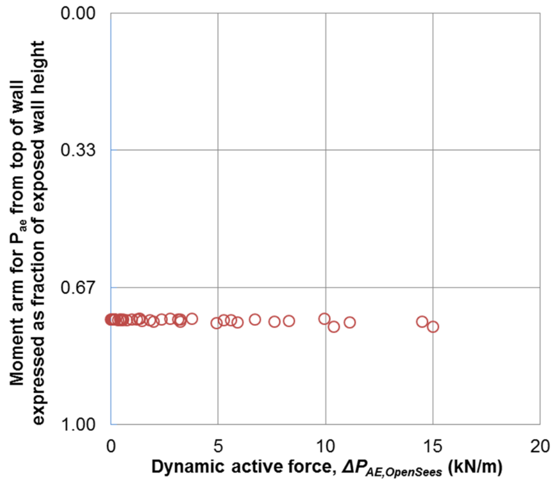

Figure 5-5 Resultant Location of $P_{ae,OpenSees}$ for NI1 Soil Class C, 0.1% ≤ ($\Delta h_{avg}/H$) < 0.2% and PGA$_{ff}$ < 0.23g

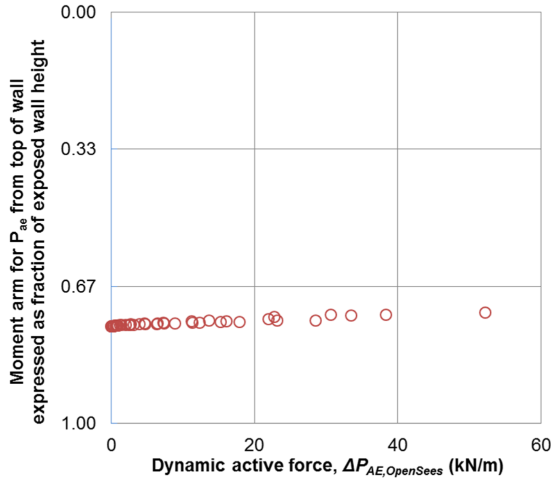

Figure 5-6 Resultant Location of $P_{ae,OpenSees}$ for NI1 Soil Class C, ($\Delta h_{avg}/H$) < 0.1% and PGA$_{ff}$ < 0.43g

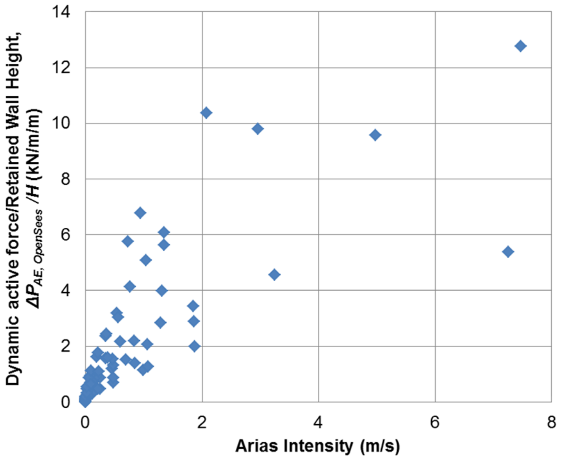

Figure 5-7 Comparison of $\Delta P_{AE,\ OpenSees}/H$ vs Arias Intensity for NI1 Soil Class C, (Δh_{avg}/H) ≥ 0.2% and PGA_{ff} < 0.7g

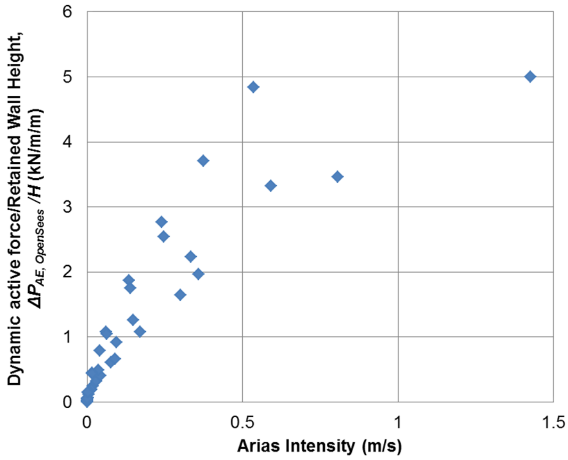

Figure 5-8 Comparison of $\Delta P_{AE,\ OpenSees}/H$ vs Arias Intensity for NI1 Soil Class C, 0.1% ≤ (Δh_{avg}/H) < 0.2% and PGA_{ff} < 0.23g

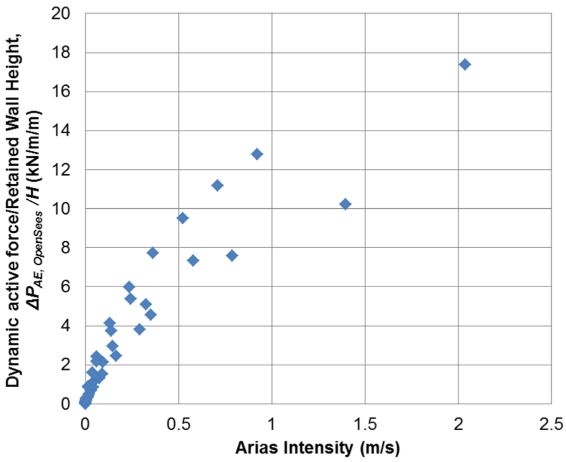

Figure 5-9 Comparison of $\Delta P_{AE,\ OpenSees}/H$ vs Arias Intensity for NI1 Soil Class C, (Δh_{avg}/H) < 0.1% and PGA_{ff} < 0.43g

5.1.2 NI1 Soil Class D

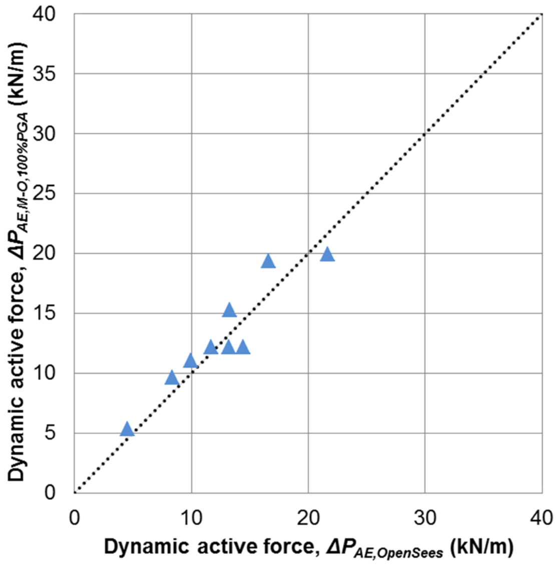

Figure 5-10 Comparison of Dynamic Active Forces $\Delta P_{AE\ OpenSees}$ vs $\Delta P_{AE,M\text{-}O,100\%PGA}$ for NI1 Soil Class D, $(\Delta h_{avg}/H) \geq 0.5\%$ and $PGA_{ff} < 0.4g$

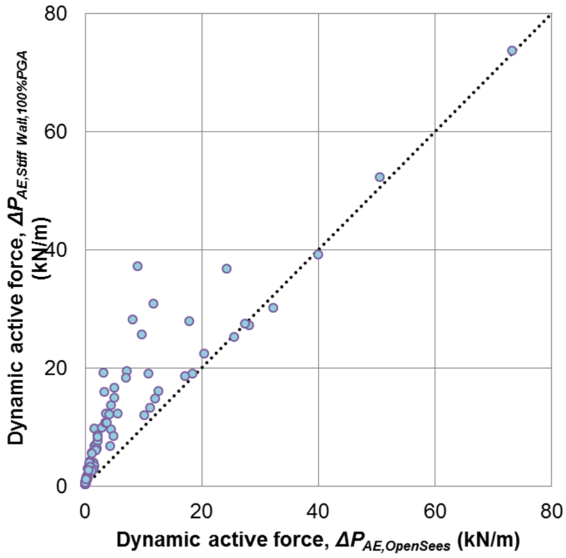

Figure 5-11 Comparison of Dynamic Active Forces $\Delta P_{AE\ OpenSees}$ vs $\Delta P_{AE,Stiff\ Wall,100\%PGA}$ for NI1 Soil Class D, $0.05\% \leq (\Delta h_{avg}/H) < 0.5\%$ and $PGA_{ff} < 0.56g$

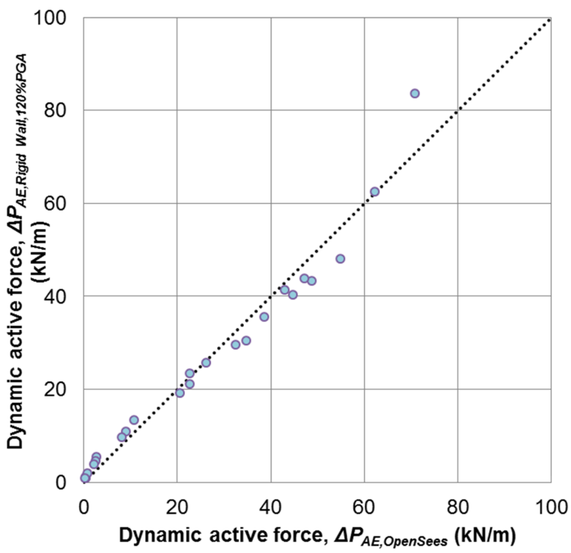

Figure 5-12 Comparison of Dynamic Active Forces $\Delta P_{AE\ OpenSees}$ vs $\Delta P_{AE,Rigid\ Wall,120\%PGA}$ for NI1 Soil Class D, $(\Delta h_{avg}/H) < 0.05\%$ and $PGA_{ff} < 0.5g$

Summary of findings for Dynamic active force $\Delta P_{AE\ OpenSees}$: NI1 Soil Class D			
Normalised average wall displacements due to both static and dynamic loads ($\Delta h_{avg}/H$) %	**Recommended Seismic coefficient (%PGA_{ff}) used in pseudo-static calculations**		
	Flexible (M-O)	**Stiff**	**Rigid**
< 0.05%	**-**	**-**	**120%**
≥ 0.05% and < 0.5%	**-**	**100%**	**-**
≥ 0.5%	**100%**	**-**	**-**

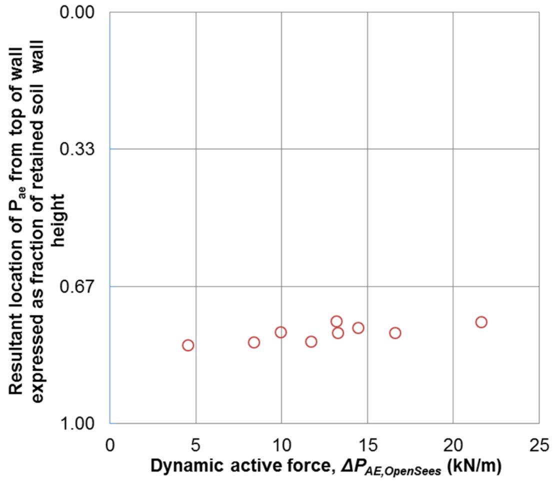

Figure 5-13 Resultant Location of $P_{ae,OpenSees}$ for NI1 Soil Class D for ($\Delta h_{avg}/H$) ≥ 0.5% and PGA$_{ff}$ < 0.4g

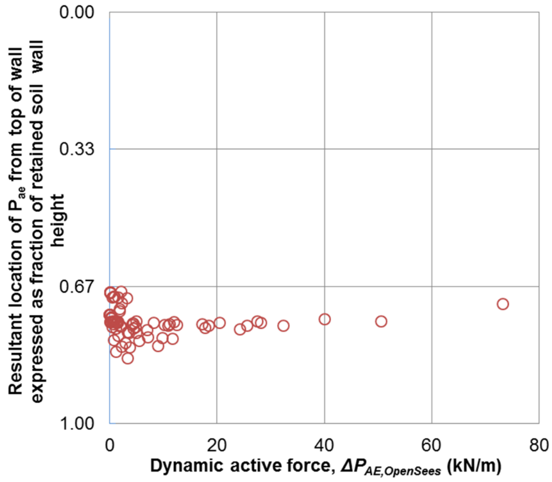

Figure 5-14 Resultant Location of $P_{ae,OpenSees}$ for NI1 Soil Class D, 0.1% ≤ ($\Delta h_{avg}/H$) < 0.5% and PGA$_{ff}$ < 0.56g

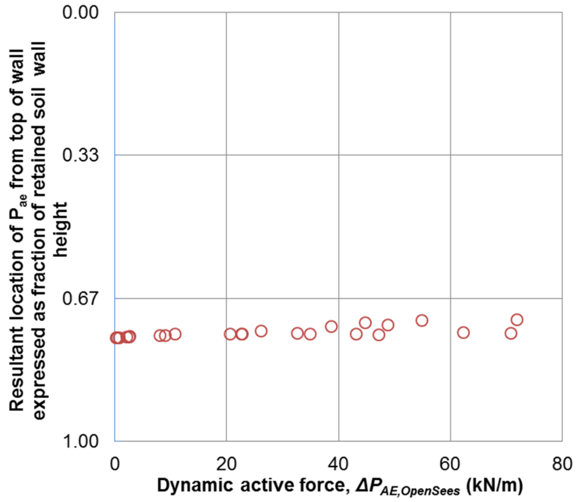

Figure 5-15 Resultant Location of $P_{ae,OpenSees}$ for NI1 Soil Class D, ($\Delta h_{avg}/H$) < 0.05% and PGA$_{ff}$ < 0.5g

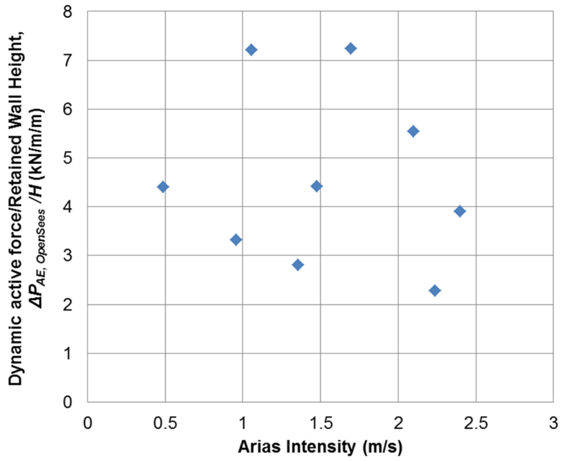

Figure 5-16 Comparison of $\Delta P_{AE,\ OpenSees}$ /H vs Arias Intensity for NI1 Soil Class D, ($\Delta h_{avg}/H$) ≥ 0.5% and PGA_{ff} < 0.4g

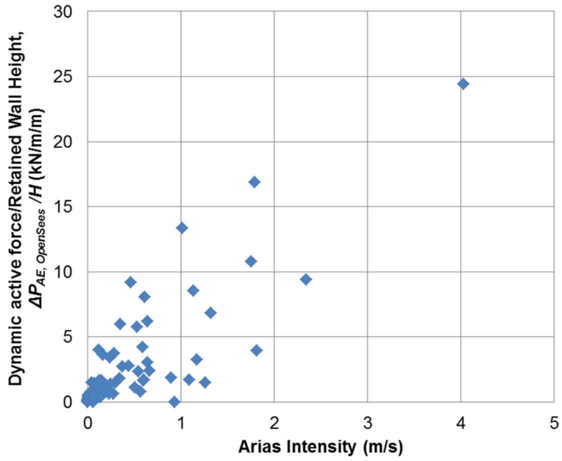

Figure 5-17 Comparison of $\Delta P_{AE,\ OpenSees}$ /H vs Arias Intensity for NI1 Soil Class D, 0.05% ≤ ($\Delta h_{avg}/H$) < 0.5% and PGA_{ff} < 0.56g

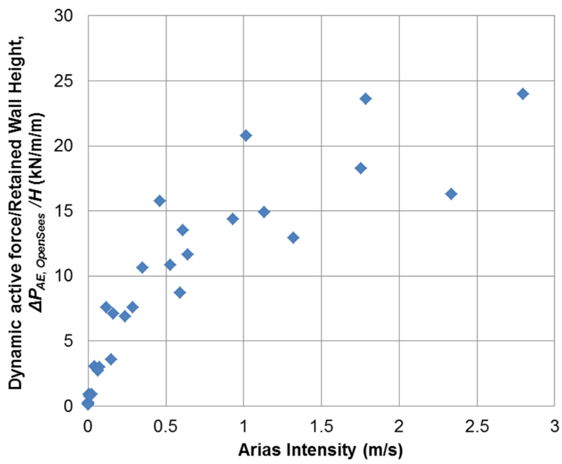

Figure 5-18 Comparison of $\Delta P_{AE,\ OpenSees}$ /H vs Arias Intensity for NI1 Soil Class D, ($\Delta h_{avg}/H$) < 0.05% and PGA_{ff} < 0.5g

5.2 North Island 2 – Wellington & Palmerston North

5.2.1 NI2 Soil Class C

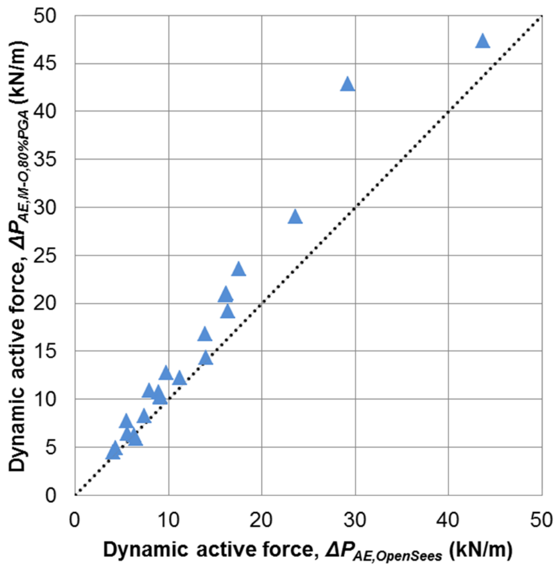

Figure 5-19 Comparison of Dynamic Active Forces $\Delta P_{AE\ OpenSees}$ vs $\Delta P_{AE,M\text{-}O,80\%PGA}$ for NI2 Soil Class C, ($\Delta h_{avg}/H$) ≥ 0.4% and PGA$_{ff}$ < 0.76g

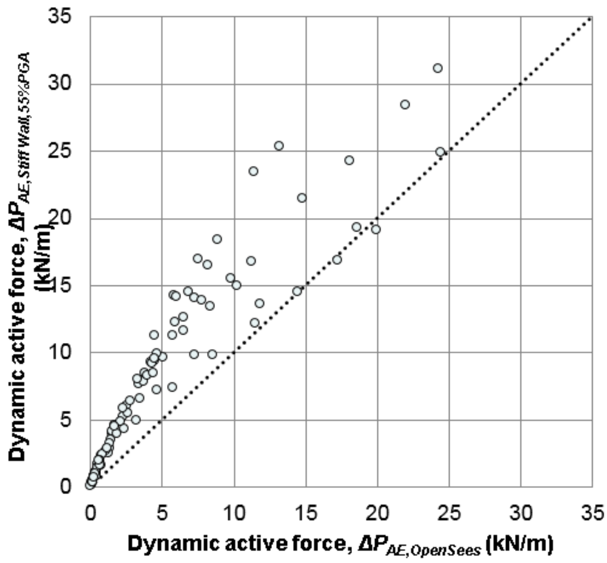

Figure 5-20 Comparison of Dynamic Active Forces $\Delta P_{AE\ OpenSees}$ vs $\Delta P_{AE,Stiff\ Wall,65\%PGA}$ for NI2 Soil Class C, 0.1% ≤ ($\Delta h_{avg}/H$) < 0.4% and PGA$_{ff}$ < 0.47g

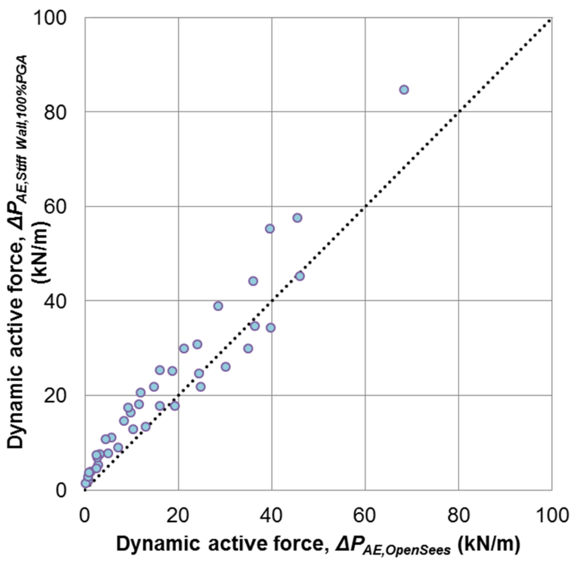

Figure 5-21 Comparison of Dynamic Active Forces $\Delta P_{AE\ OpenSees}$ vs $\Delta P_{AE,Stiff\ Wall,100\%PGA}$ for NI2 Soil Class C, ($\Delta h_{avg}/H$) < 0.1% and PGA$_{ff}$ < 0.64g

Summary of findings for Dynamic active force $\Delta P_{AE\ OpenSees}$: NI2 Soil Class C

Normalised average wall displacements due to both static and dynamic loads ($\Delta h_{avg}/H$) %	Recommended Seismic coefficient (%PGA$_{ff}$) used in pseudo-static calculations		
	Flexible (M-O)	Stiff	Rigid
< 0.1%	-	100%	-
≥ 0.1% and < 0.4%	-	55%	-
≥ 0.4%	80%	-	-

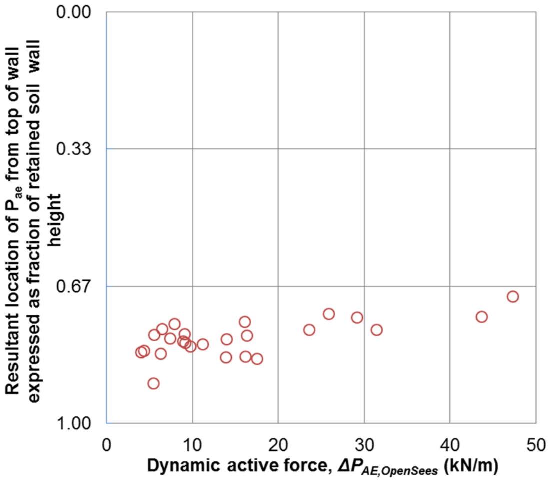

Figure 5-22 Resultant Location of $P_{ae,OpenSees}$ for NI2 Soil Class C, ($\Delta h_{avg}/H$) ≥ 0.4% and PGA$_{ff}$ < 0.76g

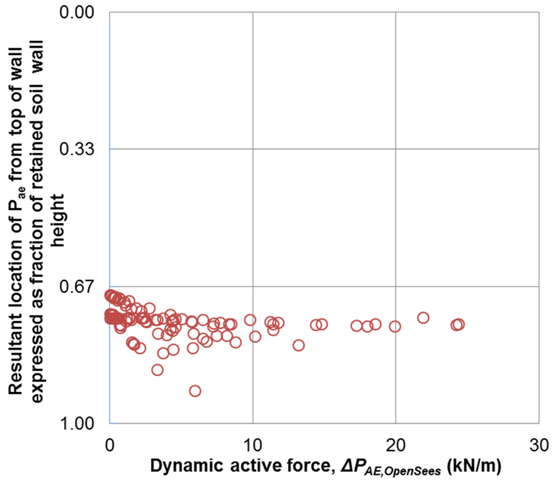

Figure 5-23 Resultant Location of $P_{ae,OpenSees}$ for NI2 Soil Class C, 0.1% ≤ ($\Delta h_{avg}/H$) < 0.4% and PGA$_{ff}$ < 0.47g

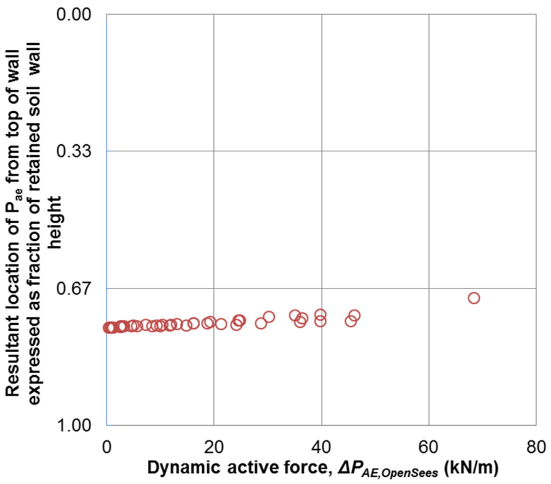

Figure 5-24 Resultant Location of $P_{ae,OpenSees}$ for NI2 Soil Class C, ($\Delta h_{avg}/H$) < 0.1% and PGA$_{ff}$ < 0.64g

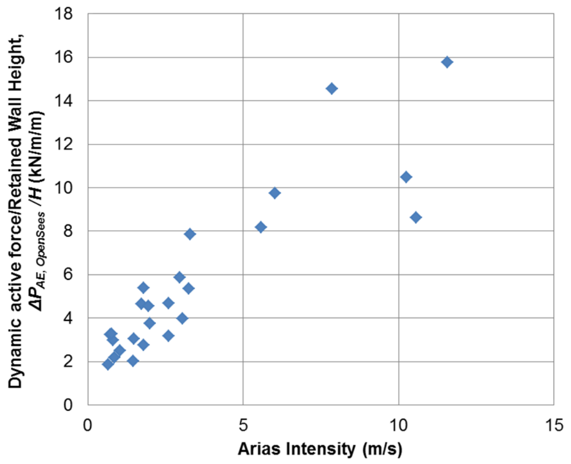

Figure 5-25 Comparison of $\Delta P_{AE,\ OpenSees}/H$ vs Arias Intensity for NI2 Soil Class C, ($\Delta h_{avg}/H$) ≥ 0.4% and PGA_{ff} < 0.76g

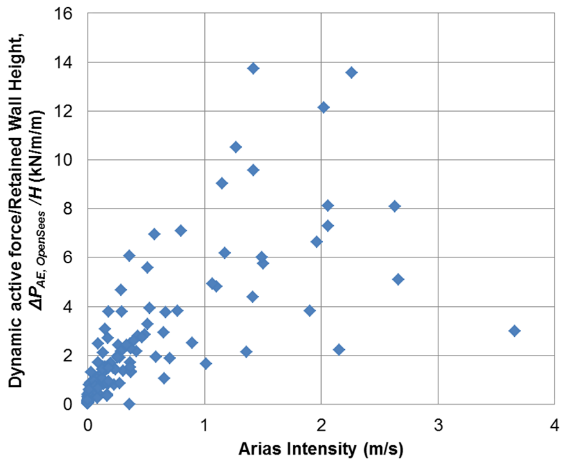

Figure 5-26 Comparison of $\Delta P_{AE,\ OpenSees}/H$ vs Arias Intensity for NI2 Soil Class C, 0.1% ≤ ($\Delta h_{avg}/H$) < 0.4% and PGA_{ff} < 0.47g

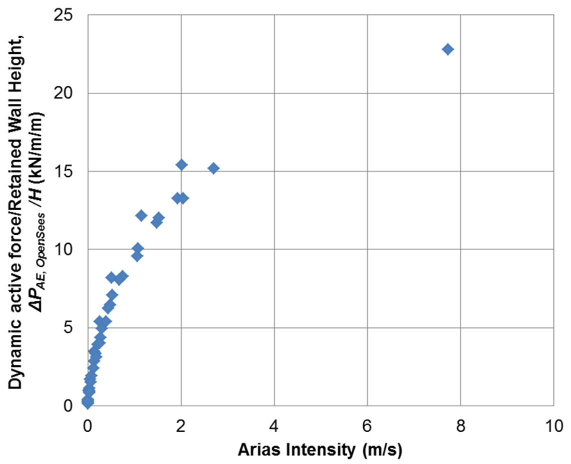

Figure 5-27 Comparison of $\Delta P_{AE,\ OpenSees}/H$ vs Arias Intensity for NI2 Soil Class C, ($\Delta h_{avg}/H$) < 0.1% and PGA_{ff} < 0.64g

5.2.2 NI2 Soil Class D

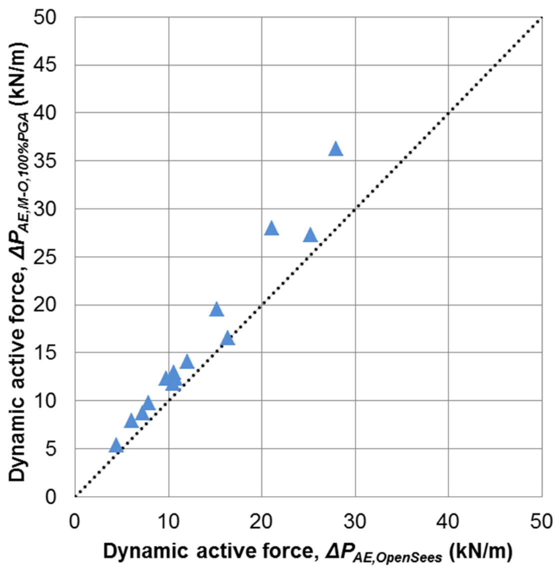

Figure 5-28 Comparison of Dynamic Active Forces $\Delta P_{AE\ OpenSees}$ vs $\Delta P_{AE,M\text{-}O,100\%PGA}$ for NI2 Soil Class D, $(\Delta h_{avg}/H) \geq 0.4\%$ and $PGA_{ff} < 0.46g$

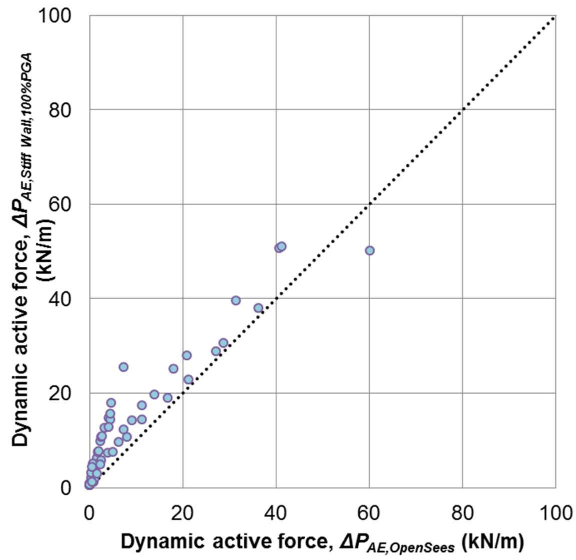

Figure 5-29 Comparison of Dynamic Active Forces $\Delta P_{AE\ OpenSees}$ vs $\Delta P_{AE,Stiff\ Wall,100\%PGA}$ for NI2 Soil Class D, $0.05\% \leq (\Delta h_{avg}/H) < 0.4\%$ and $PGA_{ff} < 0.4g$

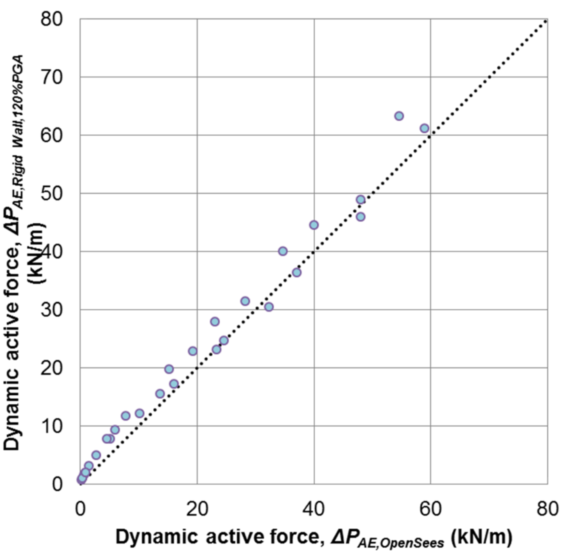

Figure 5-30: Comparison of Dynamic Active Forces $\Delta P_{AE\ OpenSees}$ vs $\Delta P_{AE,Rigid\ Wall,120\%PGA}$ for NI2 Soil Class D, $(\Delta h_{avg}/H) < 0.05\%$ and $PGA_{ff} < 0.4g$

Summary of findings for Dynamic active force $\Delta P_{AE\ OpenSees}$: NI2 Soil Class D

Normalised average wall displacements due to both static and dynamic loads ($\Delta h_{avg}/H$) %	Recommended Seismic coefficient (%PGA_{ff}) used in pseudo-static calculations		
	Flexible (M-O)	Stiff	Rigid
< 0.05%	-	-	120%
≥ 0.05% and < 0.4%	-	100%	-
≥ 0.4%	100%	-	-

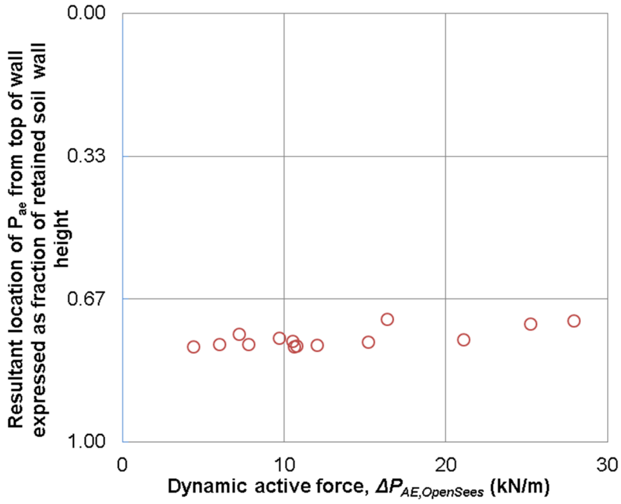

Figure 5-31 Resultant Location of $P_{ae,OpenSees}$ for NI2 Soil Class D, ($\Delta h_{avg}/H$) ≥ 0.4% and PGA$_{ff}$ < 0.46g

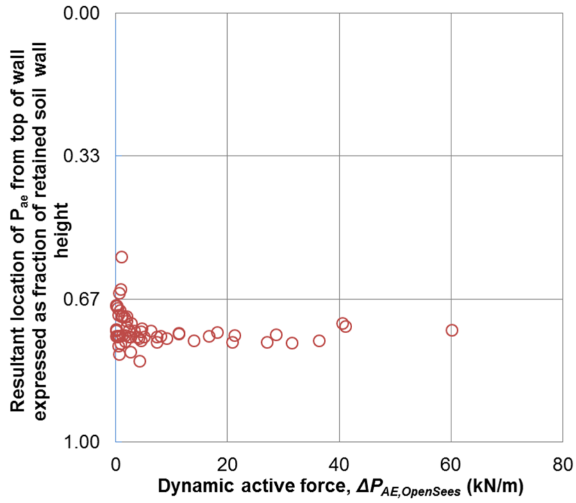

Figure 5-32 Resultant Location of $P_{ae,OpenSees}$ for NI2 Soil Class D, 0.05% ≤ ($\Delta h_{avg}/H$) < 0.4% and PGA$_{ff}$ < 0.4g

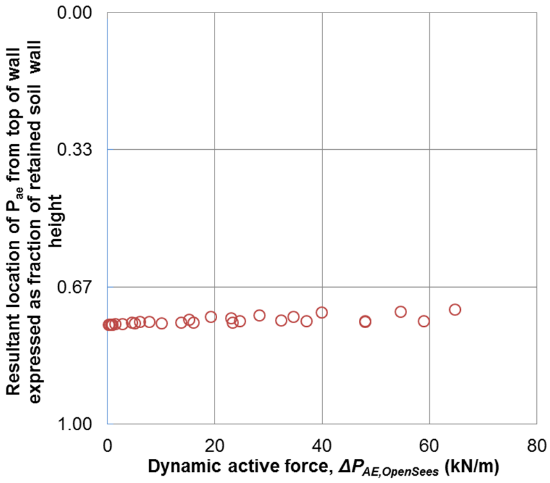

Figure 5-33 Resultant Location of $P_{ae,OpenSees}$ for NI2 Soil Class D, ($\Delta h_{avg}/H$) < 0.05% and PGA$_{ff}$ < 0.4g

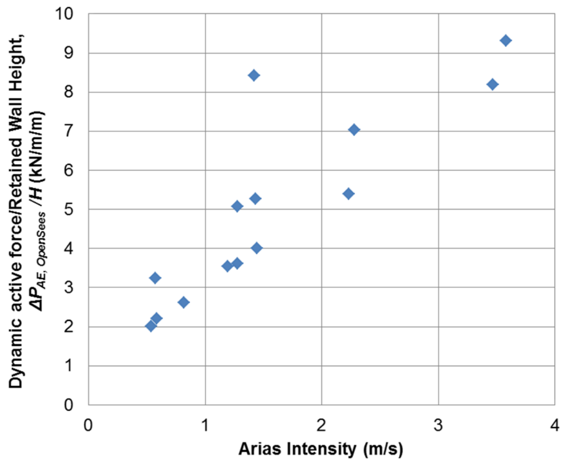

Figure 5-34 Comparison of $\Delta P_{AE,\ OpenSees}/H$ vs Arias Intensity for NI2 Soil Class D, $(\Delta h_{avg}/H) \geq 0.4\%$ and $PGA_{ff} < 0.46g$

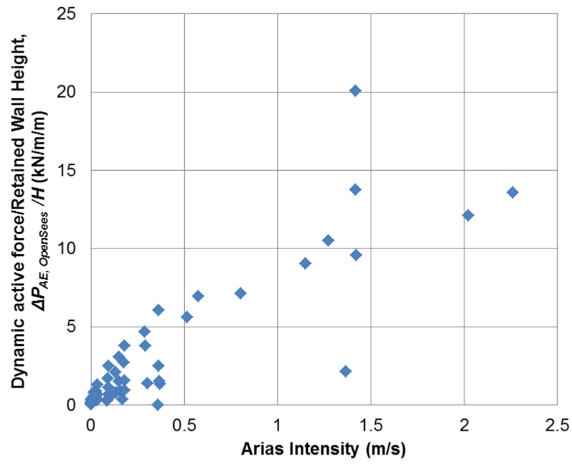

Figure 5-35 Comparison of $\Delta P_{AE,\ OpenSees}/H$ vs Arias Intensity for NI2 Soil Class D, $0.05\% \leq (\Delta h_{avg}/H) < 0.4\%$ and $PGA_{ff} < 0.4g$

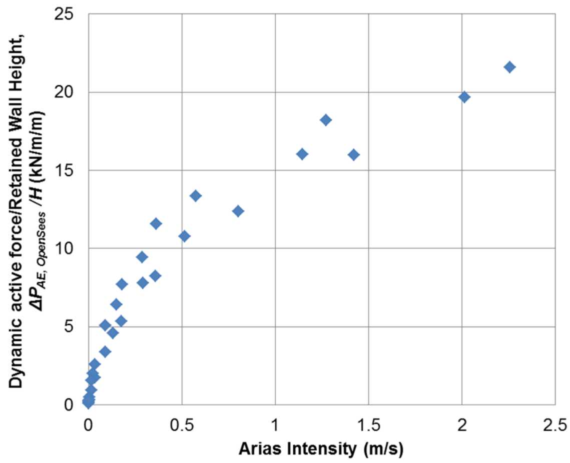

Figure 5-36 Comparison of $\Delta P_{AE,\ OpenSees}/H$ vs Arias Intensity for NI2 Soil Class D, $(\Delta h_{avg}/H) < 0.05\%$ and $PGA_{ff} < 0.4g$

5.3 South Island 1 – Christchurch

5.3.1 SI1 Soil Class C

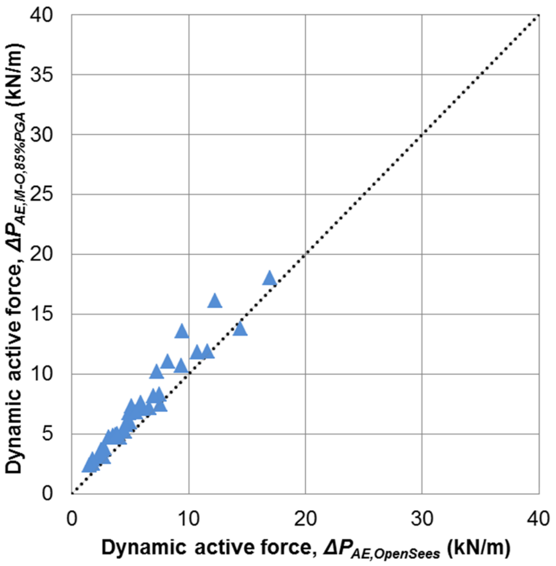

Figure 5-37 Comparison of Dynamic Active Forces $\Delta P_{AE\ OpenSees}$ vs $\Delta P_{AE,M\text{-}O,85\%PGA}$ for SI1 Soil Class C, $(\Delta h_{avg}/H) \geq 0.3\%$ and $PGA_{ff} < 0.5g$

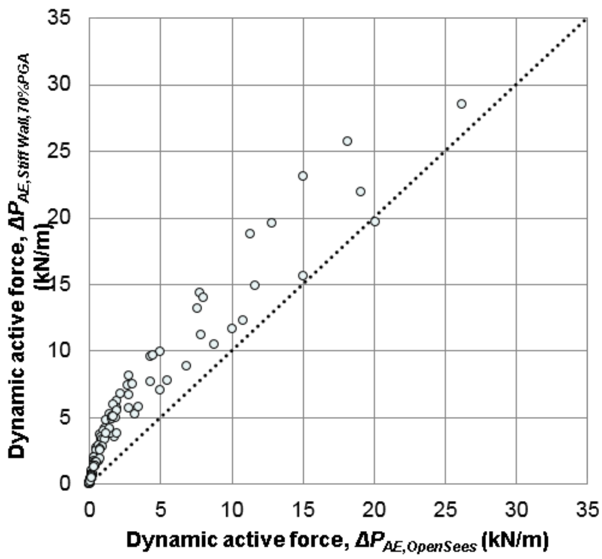

Figure 5-38 Comparison of Dynamic Active Forces $\Delta P_{AE\ OpenSees}$ vs $\Delta P_{AE,Stiff\ Wall,70\%PGA}$ for SI1 Soil Class C, $0.05\% \leq (\Delta h_{avg}/H) < 0.3\%$ and $PGA_{ff} < 0.31g$

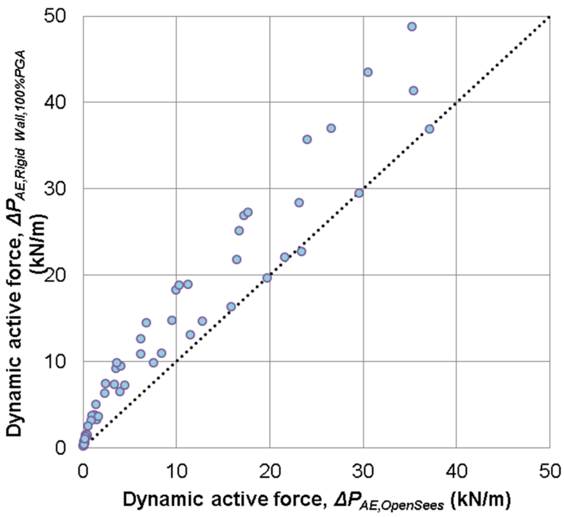

Figure 5-39 Comparison of Dynamic Active Forces $\Delta P_{AE\ OpenSees}$ vs $\Delta P_{AE,Rigid\ Wall,100\%PGA}$ for SI1 Soil Class C, $(\Delta h_{avg}/H) < 0.05\%$ and $PGA_{ff} < 0.31g$

Summary of findings for Dynamic active force $\Delta P_{AE\ OpenSees}$: SI1 Soil Class C			
Normalised average wall displacements due to both static and dynamic loads ($\Delta h_{avg}/H$) %	**Recommended Seismic coefficient (%PGA_{ff}) used in pseudo-static calculations**		
	Flexible (M-O)	**Stiff**	**Rigid**
< 0.05%	-	-	**100%**
≥ 0.05% and < 0.3%	-	**70%**	-
≥ 0.3%	**85**	-	-

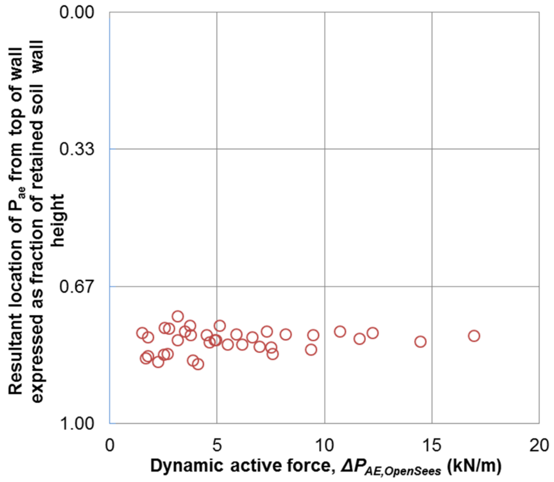

Figure 5-40 Resultant Location of $P_{ae,OpenSees}$ for SI1 Soil Class C, ($\Delta h_{avg}/H$) ≥ 0.3% and PGA$_{ff}$ < 0.5g

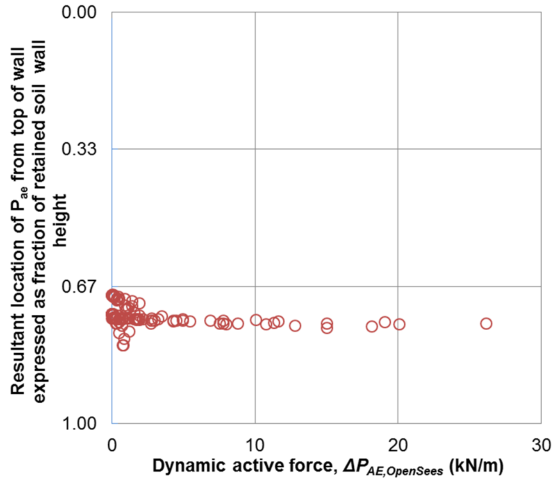

Figure 5-41 Resultant Location of $P_{ae,OpenSees}$ for SI1 Soil Class C, 0.05% ≤ ($\Delta h_{avg}/H$) < 0.3% and PGA$_{ff}$ < 0.31g

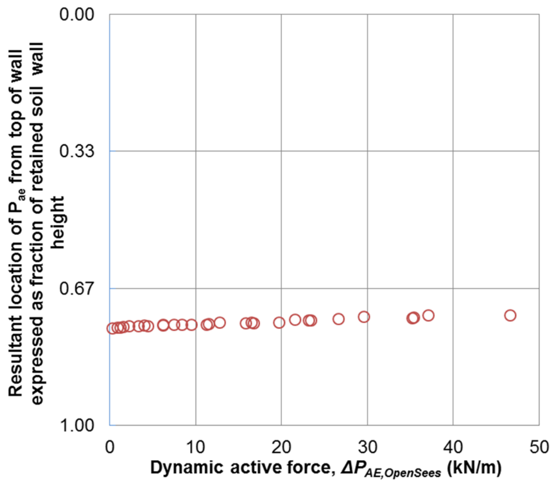

Figure 5-42 Resultant Location of $P_{ae,OpenSees}$ for SI1 Soil Class C, ($\Delta h_{avg}/H$) < 0.05% and PGA$_{ff}$ < 0.31g

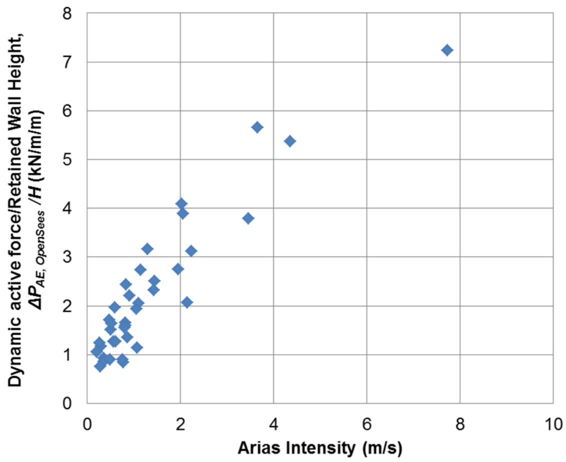

Figure 5-43 Comparison of $\Delta P_{AE,\ OpenSees}/H$ vs Arias Intensity for SI1 Soil Class C, $(\Delta h_{avg}/H) \geq 0.3\%$ and $PGA_{ff} < 0.5g$

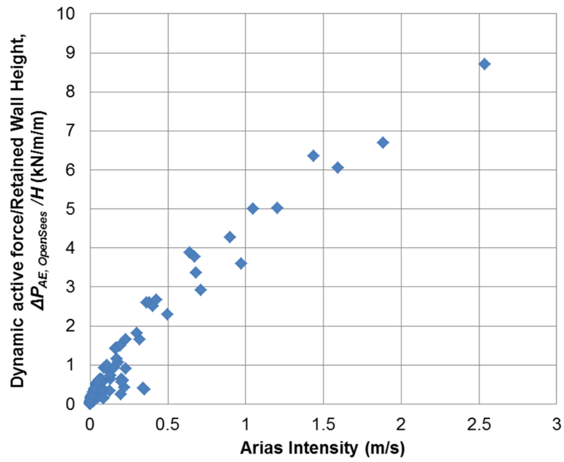

Figure 5-44 Comparison of $\Delta P_{AE,\ OpenSees}/H$ vs Arias Intensity for SI1 Soil Class C, $0.05\% \leq (\Delta h_{avg}/H) < 0.3\%$ and $PGA_{ff} < 0.31g$

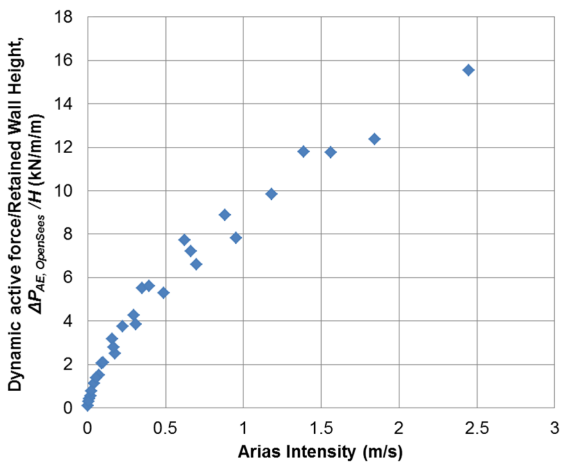

Figure 5-45 Comparison of $\Delta P_{AE,\ OpenSees}/H$ vs Arias Intensity for SI1 Soil Class C, $(\Delta h_{avg}/H) < 0.05\%$ and $PGA_{ff} < 0.31g$

5.3.2 SI1 Soil Class D

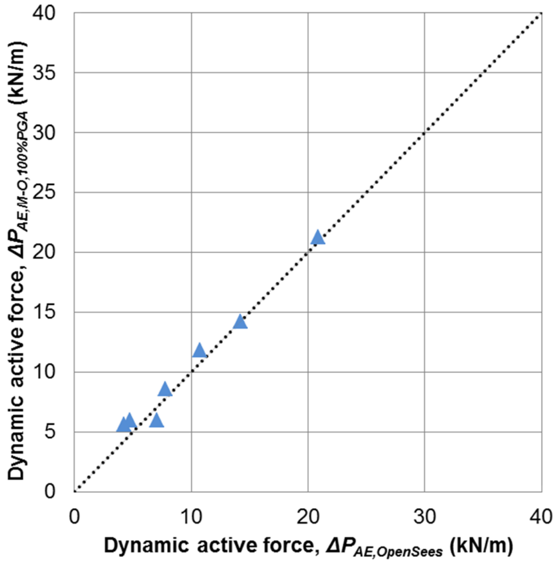

Figure 5-46 Comparison of Dynamic Active Forces $\Delta P_{AE\ OpenSees}$ vs $\Delta P_{AE,M\text{-}O,100\%PGA}$ for SI1 Soil Class D, ($\Delta h_{avg}/H$) ≥ 0.5% and PGA$_{ff}$ < 0.38g

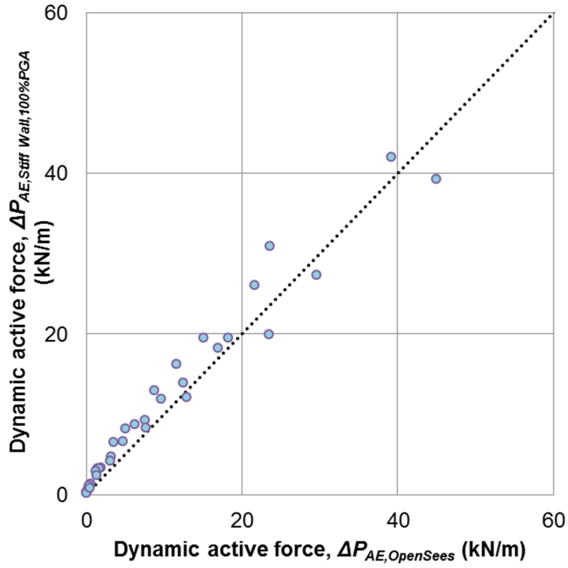

Figure 5-47 Comparison of Dynamic Active Forces $\Delta P_{AE\ OpenSees}$ vs $\Delta P_{AE,Stiff\ Wall,100\%PGA}$ for SI1 Soil Class D, 0.05% ≤ ($\Delta h_{avg}/H$) < 0.5% and PGA$_{ff}$ < 0.32g

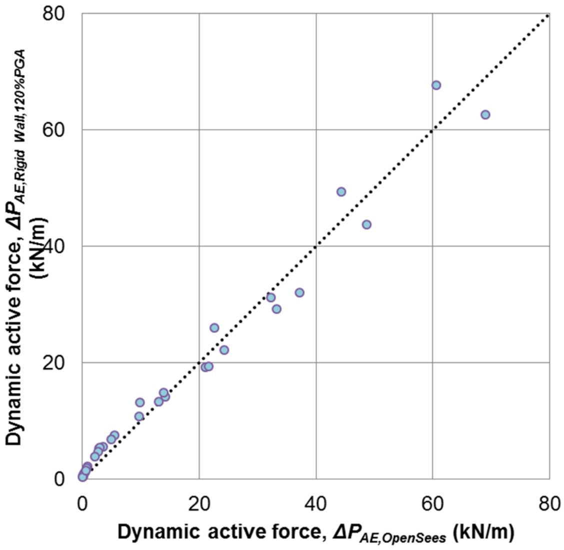

Figure 5-48 Comparison of Dynamic Active Forces $\Delta P_{AE\ OpenSees}$ vs $\Delta P_{AE,Rigid\ Wall,120\%PGA}$ for SI1 Soil Class D, ($\Delta h_{avg}/H$) < 0.05% and PGA$_{ff}$ < 0.32g

Summary of findings for Dynamic active force $\Delta P_{AE\ OpenSees}$: SI1 Soil Class D

Normalised average wall displacements due to both static and dynamic loads ($\Delta h_{avg}/H$) %	Recommended Seismic coefficient (%PGA$_{ff}$) used in pseudo-static calculations		
	Flexible (M-O)	Stiff	Rigid
< 0.05%	-	-	120%
≥ 0.05% and < 0.5%	-	100%	-
≥ 0.5%	100%	-	-

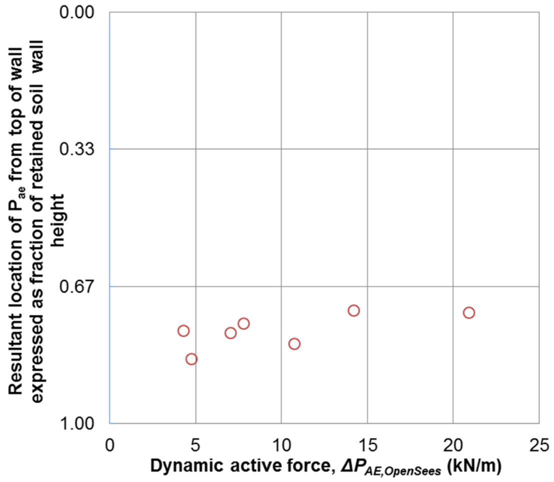

Figure 5-49 Resultant Location of $P_{ae,OpenSees}$ for SI1 Soil Class D for ($\Delta h_{avg}/H$) ≥ 0.5% and PGA$_{ff}$ < 0.38g

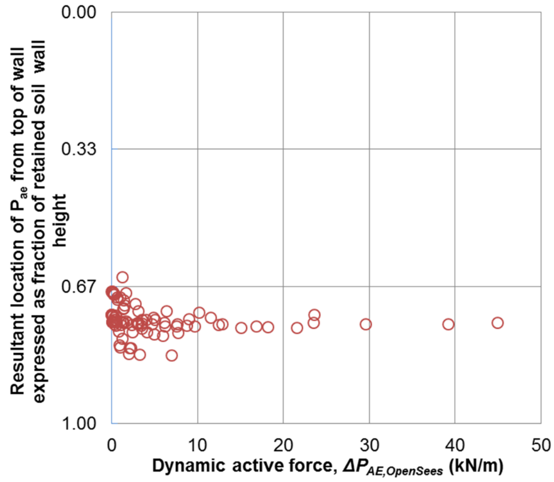

Figure 5-50 Resultant Location of $P_{ae,OpenSees}$ for SI1 Soil Class D, 0.05% ≤ ($\Delta h_{avg}/H$) < 0.5% and PGA$_{ff}$ < 0.32g

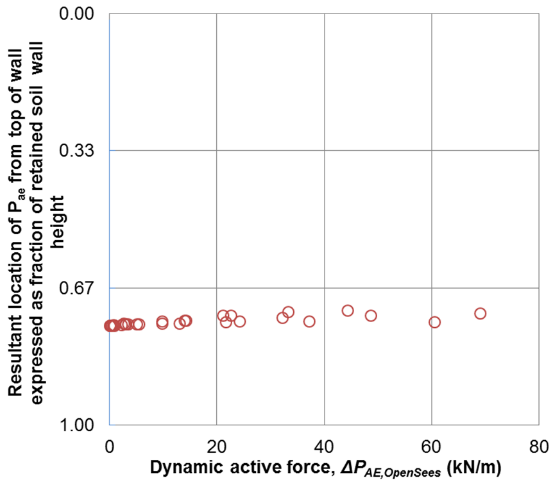

Figure 5-51 Resultant Location of $P_{ae,OpenSees}$ for SI1 Soil Class D, ($\Delta h_{avg}/H$) < 0.05% and PGA$_{ff}$ < 0.32g

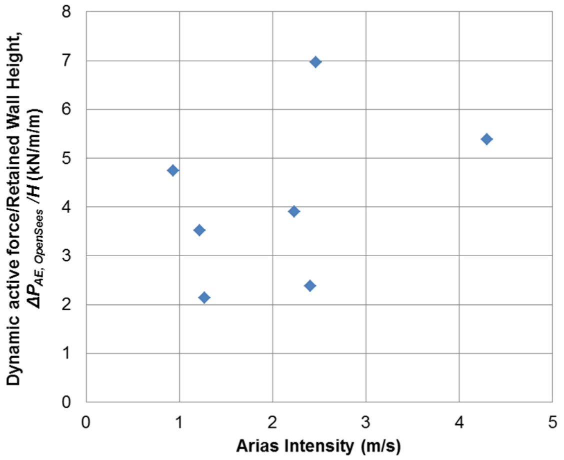

Figure 5-52 Comparison of $\Delta P_{AE,\ OpenSees}/H$ vs Arias Intensity for SI1 Soil Class D, $(\Delta h_{avg}/H) \geq 0.5\%$ and $PGA_{ff} < 0.38g$

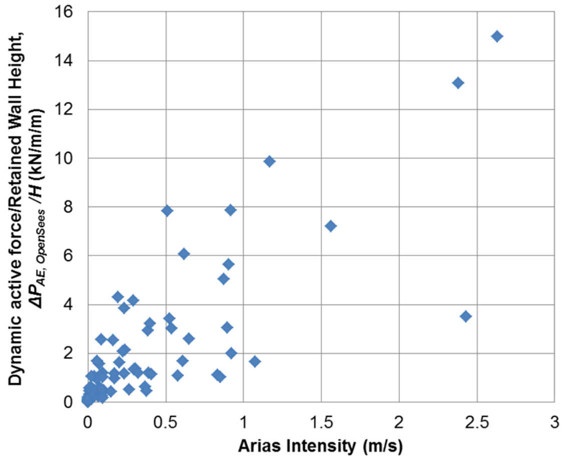

Figure 5-53 Comparison of $\Delta P_{AE,\ OpenSees}/H$ vs Arias Intensity for SI1 Soil Class D, $0.05\% \leq (\Delta h_{avg}/H) < 0.5\%$ and $PGA_{ff} < 0.32g$

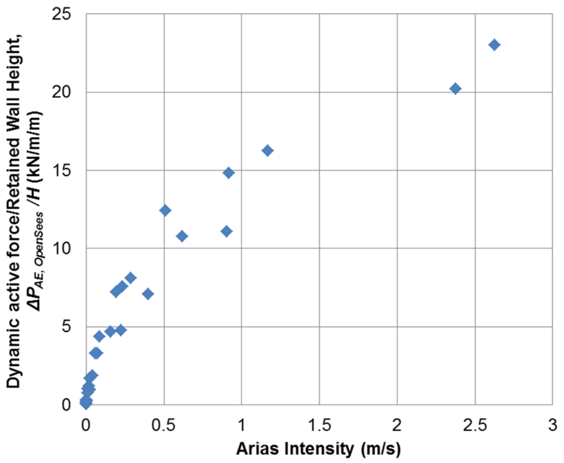

Figure 5-54 Comparison of $\Delta P_{AE,\ OpenSees}/H$ vs Arias Intensity for SI1 Soil Class D, $(\Delta h_{avg}/H) < 0.05\%$ and $PGA_{ff} < 0.32g$

5.4 Recommended Seismic Coefficient used in Pseudo-Static calculations

Based on the results of 946 dynamic non-linear OpenSees analyses, the following recommendations for fractions of PGA_{ff} used in simplified pseudo-static methods can be made. The pseudo-static methods referred to in the table below are the Flexible (M-O), Stiff and Rigid wall methods (Section 2.1).

Table 5-1 Recommended Seismic Coefficient for use in Pseudo-Static Analysis

Geographical location	Soil class	Normalised average wall displacements due to static & dynamic loads ($\Delta h_{avg}/H$)%	Recommended Seismic coefficient (%PGA_{ff}) used in pseudo-static calculations		
			Flexible (M-O)	Stiff	Rigid
North Island 1	C	< 0.1%	-	100%	-
		≥ 0.1% and < 0.2%	-	55%	-
		≥ 0.2%	85%	-	-
	D	< 0.05%	-	-	120%
		≥ 0.05% and < 0.5%	-	100%	
		≥ 0.5%	100%	-	-
North Island 2	C	< 0.1%	-	100%	-
		≥ 0.1% and < 0.4%	-	55%	-
		≥ 0.4%	80%	-	-
	D	< 0.05%	-	-	120%
		≥ 0.05% and < 0.4%	-	100%	-
		≥ 0.4%	100%	-	-
South Island 1	C	< 0.05%	-	-	100%
		≥ 0.05% and < 0.3%	-	70%	-
		≥ 0.3%	85%	-	-
	D	< 0.05%	-	-	120%
		≥ 0.05% and < 0.5%	-	100%	-
		≥ 0.5%	100%	-	-

It is clear from interpreting the OpenSees results (Sections 0 to 5.3) that the dynamic active force (ΔP_{AE}) is a function of wall displacements. An opportunity to revise the displacement criteria from "top of wall" (as suggested by Matthewson et al., 1980 and Wood & Elms, 1990) to an average wall displacement over the height of the retained soil was taken. This was undertaken to address the issue that maximum displacements do not necessarily always occur at the top of wall (commonly in propped walls) and also to acknowledge that the overall displaced profile of the wall, rather than the displacement at the top of the wall greatly affects the resultant dynamic active force.

5.5 General Comments

Results from OpenSees indicate that resultant locations of the total dynamic active force, P_{AE} (comprising both static and dynamic forces) typically act at 0.7*H* (where *H* is the retained soil height) from the top of the wall. This agrees approximately with the 2/3rd *H* recommendation of Wood & Elms (1990) and also with Atik & Sitar (2008, 2010).

An assessment of the times at which the maximum PGA_{ff} occurred compared to when the maximum dynamic active force occurred was carried out (Figure 5-55). This showed that in ~80% of all the runs, the occurrences of maximum PGA_{ff} and $\Delta P_{AE,\ OpenSees}$ did not coincide. In the majority of the cases, maximum $\Delta P_{AE,\ OpenSees}$ occurred after the occurrence of maximum PGA_{ff}.

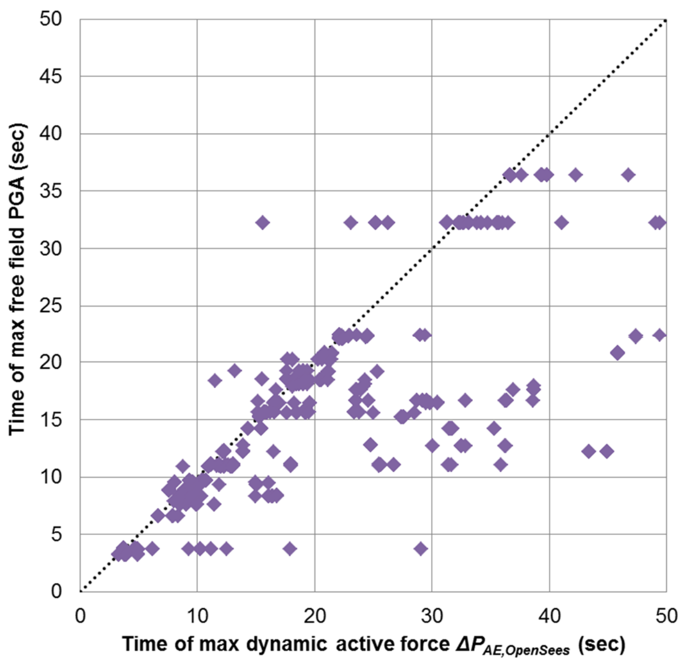

Figure 5-55: Comparison of Times of Occurrence of Maximum PGA_{ff} & $\Delta P_{AE,\ OpenSees}$

An assessment of the times at which the maximum PGA_{ff} occurred compared to when the maximum wall bending moment occurred was also carried out (Figure 5-56). This showed that in ~72% of all the runs, the occurrences of maximum PGA_{ff} did not coincide with the time of maximum bending moment.

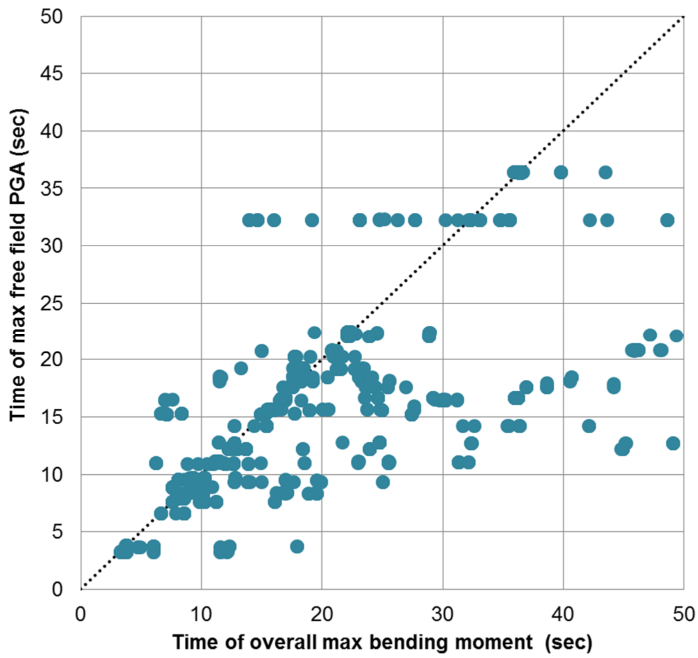

Figure 5-56: Comparison of Times of Occurrence of Maximum PGA_{ff} & Maximum Wall Bending Moment

In ~68% of all the runs, the times at which maximum dynamic active force, ΔP_{AE}, occurred did not coincide with the times at which maximum wall bending moment occurred (Figure 5-57). A similar finding was reported in centrifuge test results by Atik & Sitar (2010), who attributed this to out of phase soil and wall displacements.

Although it could be considered conservative to assume the concurrence of maximum dynamic active force with maximum bending moment, this assumption is recommended on the basis that in some 32% of the runs, this occurrence took place.

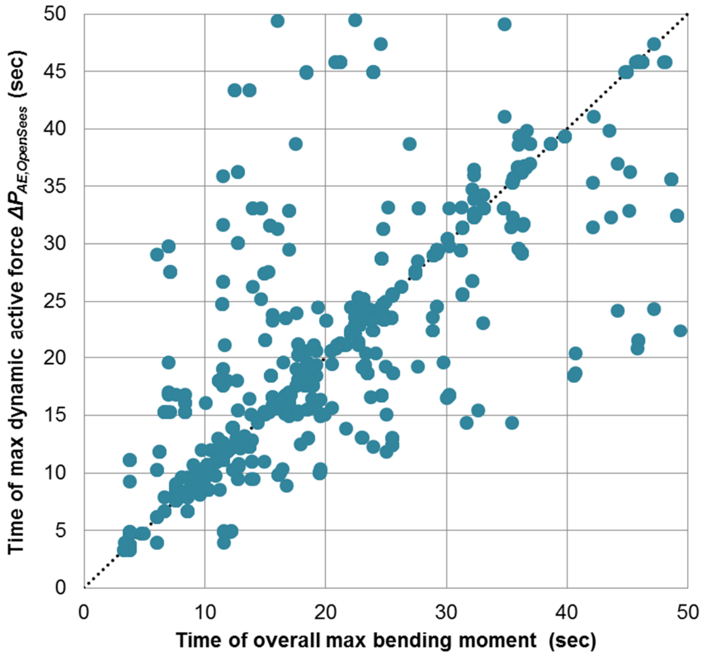

Figure 5-57: Comparison of Times of Occurrence of Maximum $\Delta P_{AE,\ OpenSees}$ and Maximum Wall Bending Moment

6 Conclusion

This study has used a two-dimensional non-linear dynamic finite element program, OpenSees to determine seismic soil thrusts acting on retaining walls. The three main objectives of this study were to investigate the following:-

1. Compare seismic soil thrusts from OpenSees modelling against pseudo-static analytical methods such as the Rigid, Stiff and Flexible wall solutions & determine if a reduction (or increase) to free-field PGA, applied as a seismic coefficient to these solutions, can be justified.

2. Identify the range of wall displacements applicable to the pseudo-static solutions.

3. Determine the location of seismic active soil thrust acting on the retaining wall.

The above study was limited to three geographical zones in New Zealand. These are described in the report as:-

1. North Island 1 (NI1) which includes Auckland, Hamilton & New Plymouth.

2. North Island 2 (NI2) which includes Wellington & Palmerston North.

3. South Island 1 (SI1) which covers Christchurch.

OpenSees was used to model embedded cantilever and propped retaining walls in two different soil classes (Table 3-1). These soil classes were Class C (shallow soils) and Class D (deep soils) in accordance with New Zealand Standard 1170.5 (NZS 1170.5:2004).

As is commonly used in the study of seismic actions on structures (e.g., NZS 1170.5:2004 clause 5.5), a suite of appropriate acceleration-time histories appropriate for the above three geographical zones and soil class were established for this study (Table 4-1, Table 4-2 and Table 4-3). These motions were deconvoluted from the ground surface to the base of the model using one-dimensional equivalent linear analysis (STRATA, 2013) and subsequently integrated to provide velocity-time history records applied to the base of the OpenSees model. Additional scaling of the deconvoluted acceleration amplitudes were carried out to model varying amplitudes of motions. A total of 946 runs were conducted in OpenSees

To account for non-linearity in the soil's response to seismic loading, a variation of the Pressure Dependent Multi-Yield constitutive material (PDMY02) was used to model soil in OpenSees. This allowed for elastic-plastic behaviour simulating a non-linear stress-strain relationship (Section 3.2). The model was based on dry soil with no liquefaction.

Results of seismic soil thrusts from OpenSees analyses and the three pseudo-static methods showed some interesting correlations. These demonstrated that by using the correct fraction of free-field PGA (Table 5-1), pseudo-static methods can be used to determine moderately conservative estimates of the maximum seismic soil thrust subject to the appropriate wall displacement response. Hence, the current industry-standard method of carrying out a series of iterative calculations which match the assumed wall displacement associated with a particular pseudo-static method with the derived wall displacement remains a reasonable way to carry out this analysis.

This study has established the sensitivity of the maximum seismic soil thrust to average wall displacements. For each of the geographical zones and soil classes studied, the maximum seismic soil thrust could be attributed to different ranges of wall displacements. The total dynamic active force was found to act typically at 0.7*H* (where *H* is the retained soil height) from the top of the wall.

It is recommended that until further evidence becomes available, a reasonably conservative design approach would be to include inertial loading of the wall acting concurrently with the maximum dynamic active forces recommended in this study.

It is important to note that the results presented in this study should be considered to be applicable only within the parameters considered. It is clear, for example, that changes in soil properties behind the retaining wall could generate different results. Additional research incorporating other variations in parameters such as wall heights, wall types and walls sited on slopes would be very beneficial.

7 References

Anderson, D.G., Martin, G.R., Lam, I. & Wang, J.N. (2008). National Cooperative Highway Research Program Report 611. Seismic analysis and design of retaining walls, buried structures, slopes and embankments.

Arias, A. (1970). A measure of earthquake intensity, R.J. Hansen, ed. Seismic design for nuclear power plants, MIT Press, Cambridge, Massachusetts, pp. 438 – 483.

Atik, L.A. & Sitar, N. (2008). Pacific Earthquake Engineering Research Center 2008/104. Experimental and analytical study of the seismic performance of retaining structures.

Atik, L.A. & Sitar, N. (2010). Seismic earth pressures on cantilever retaining structures. Journal of Geotechnical and Geoenvironmental Engineering ASCE, 136 (10), pp. 1324 –1333.

Gazetas, G., Psarropoulos, P.N., Anastasopoulos, I., & Gerolymos, N. (2004). Seismic behaviour of flexible retaining systems subjected to short-duration moderately strong excitation. Soil Dynamic and Earthquake Engineering, 24, pp. 537 – 550.

Greek Regulatory Guide E39/93 (1998). Regulatory guide E39/93 for the seismic analysis of bridges (Ministry of Public Works). Bulletin of Greek Technical Chamber, No. 2040, 1998.

Green, R.A., Olgun, C.G., Ebeling, R.M. & Cameron, W.I. (2003). Seismically induced lateral earth pressures on a cantilever retaining wall. Proceedings 6th U.S. Conference and Workshop on Lifeline Earthquake Engineering, Long Beach, Calif.

Kuhlemeyer, R.L. & Lysmer, J. (1973). Finite element accuracy for wave propagation problems (Technical note). Journal of Soil Mechanics and Foundations Division, Proc. ASCE, 99, SM5, 421-427.

McGann, C.R., Arduino, P. & Mackenzie-Helnwein, P. (2012). Stabilized single-point 4-node quadrilateral element for dynamic analysis of fluid saturated porous media. Acta Geotechnica, 7(4), 297-311.

McGann, C.R. & Arduino, P. (2015). Dynamic 2D Effective Stress Analysis of Slope, accessed 08 September 2015, http://opensees.berkeley.edu/wiki/index.php/Dynamic_2D_Effective_Stress_Analysis_of_Slope

Matthewson, M.B., Wood, J.H. & Berrill, J.B. (1980). Seismic design of bridges – Earth retaining structures. Bulletin NZ National Society of Earthquake Engineering, 13(3), pp. 280 – 293.

Mejia, L.H. & Dawson, E.M. (2006). Earthquake deconvolution for FLAC. 4th International FLAC symposium on numerical modelling in Geomechanics. Hart & Varona (eds.).

Mononobe, N. & Matsuo, M. (1929). On the determination of earth pressures during earthquakes. Proceedings World Engineering Congress, 9, pp. 179 – 187.

NZS 1170.5:2004. New Zealand Standard. Structural design actions Part 5: Earthquake actions – New Zealand.

NZTA Bridge Manual (2014). NZ Transport Agency Bridge Manual; Manual number SP/M/022, 3rd Edition, Amendment 1, September 2014.

Ohta, Y. & Goto, N. (1978). Empirical shear wave velocity equations in terms of characteristic soil indexes. Earthquake Engineering & Structural Dynamics, 6 (2), pp. 167-187.

Okabe, S. (1926). General theory of earth pressures. Journal of Japan Society of Civil Engineers, 12(1), pp. 123 – 134.

Oyarzo-Vera, C., McVerry, G.H. & Ingham, J.M. (2012). Seismic zonation and default suite of ground-motion records for time-history analysis in the North Island of New Zealand. Earthquake Spectra, 28(2), pp. 667 – 688.

Parra-Colmenares, E.J. (1996). Numerical modeling of liquefaction and lateral ground deformation including cyclic mobility and dilation response in soil systems. PhD Thesis, Rensselaer Polytechnic Institute, Troy, NY.

Psarropoulos, P.N., Klonaris, G., & Gazetas, G. (2005). Seismic earth pressures on rigid and flexible retaining walls. International Journal of Soil Dynamics and Earthquake Engineering, 25, pp. 795 – 809.

Rathje, E.M., Faraj, F., Russell, S. & Bray, J. (2004). Empirical relationships for frequency content parameters of earthquake ground motions. Earthquake Spectra, 20(1), pp. 119 - 144. February 2004, Earthquake Engineering Research Institute.

Scott, M.H. & Fenves, G.L. (2010). A Krylov subspace accelerated Newton algorithm: Application to dynamic progressive collapse simulation of frames. Journal of Structural Engineering, 136(5).

Smith, W.D. (1975). The application of finite element analysis to body wave propagation problems. Geophysical Journal of the Royal Astronomical Society, 42, pp. 747 – 768.

Steedman, R.S. & Zeng, X. (1990). The influence of phase on the calculation of pseudo-static earth pressure on a retaining wall. Geotechnique 40(1), pp. 103 – 112.

STRATA (2013). Rathje, E.M. & Kottke, A., accessed 08 September 2015, https://nees.org/resources/strata

Tarbali, K. & Bradley, B.A. (2014). Representative ground-motion ensembles for several major earthquake scenarios in New Zealand. Bulletin of the New Zealand Society for Earthquake Engineering, 47(4), December 2014.

Wood, J.H. (1973). Earthquake-induced soil pressures on structures. PhD Thesis, California Institute of Technology, Pasadena, California.

Wood, J.H. & Elms, D.G. (1990). Seismic design of bridge abutments and retaining walls. Transit New Zealand Road Research Unit Bulletin 84 Volume 2.

Yang, Z. (2000). Numerical modeling of earthquake site response including dilation and liquefaction. PhD Thesis, Columbia University.

Yang, Z., Lu, J. & Elgamal, A. (2008). OpenSees soil models and solid-fluid fully coupled elements. User's manual. 2008 ver 1.0. University of California, San Diego.

Zhang, Y., Conte, J.P., Yang, Z., Elgamal, A., Bielak, J. & Acero, G. (2008). Two-dimensional nonlinear earthquake response analysis of a bridge-foundation-ground system. Earthquake Spectra (24)2, pp. 343-386, Earthquake Engineering Research Institute.

Appendix A – Summary of OpenSees Runs

In total, 946 dynamic analyses were conducted using OpenSees. These are listed below.

The nomenclatures of file names adopted are as follows:-

A_Bbb_Ccc_Ddd_Ee_Fff

A: Refers to the Soil Class

C: Soil Class C

D: Soil Class D

Bbb: Refers to the geographical location (Refer to Section 4.2)

NI1: North Island 1

NI2: North Island 2

SI1: South Island 1

Ccc: Refers the acceleration-time history used in the analysis (Refer to Table 4-1, Table 4-2 and Table 4-3, Section 4)

Bov:	Bovino, Campano Lucano, Italy
Cal:	Caleta de Campos, Mexico
Chi:	Chi-Chi, Taiwan
Cor:	Corinthos, Greece
Del:	Delta, Imperial Valley, USA
Duz:	Duzce, Turkey
El6:	El Centro #6, Imperial Valley, USA
Elc:	El Centro, Imperial Valley, USA
Hec:	Hector Mine
Kal:	Kalamata, Greece
Koc:	Arcelik, Kocaeli, Turkey
Lan:	Landers
Lau:	La Union, Mexico
Luc:	Lucerne, landers, USA
Mat:	Matahina Dam D, Edgecumbe, NZ
Nor:	Northridge-01
San:	San Fernando
Tab:	Tabas, Iran
Wes:	Westmorland, USA
Yar:	Yarimka YPT, Kocaeli, Turkey

Ddd: Refers to the fraction applied to the deconvoluted acceleration-time history. Examples of some fractions are:-

1.00: A multiplier of 1.00 is applied to the deconvoluted original acceleration-time history (i.e., unfactored)

0.50: A multiplier of 0.50 is applied to the deconvoluted original acceleration-time history

Ee: Refers to the retained soil height of the wall in meters. Examples of this are:-

2m: A 2m retained soil height

3m: A 3m retained soil height

Fff: Refers to the type of wall

[Blank]: Cantilever embedded wall

2P: Double propped wall, prop stiffness 1, Type 2P (Refer to Section 3.3)

2Pa: Double propped wall, prop stiffness 2, Type 2Pa (Refer to Section 3.3)

Examples: **C_NI1_Bov_1.00_2m_** would refer to an OpenSees analysis for

- Soil Class C
- North Island 1
- Bovino, Campano Lucano, Italy acceleration-time history
- 1.00 times (i.e., unfactored) the amplitude of the deconvoluted acceleration-time history
- 2m retained soil height
- Embedded cantilever wall

D_SI1_Koc_0.50_3m_2Pa. would refer to an OpenSees analysis for

- Soil Class D
- South Island 1
- Arcelik, Kocaeli, Turkey acceleration-time history
- 0.50 times the amplitude of the deconvoluted acceleration-time history
- 3m retained soil height
- Type 2Pa double propped wall

Number	OpenSees Run Name
1	C_NI1_Bov_0.02_3m_
2	C_NI1_Bov_0.02_3m_2P
3	C_NI1_Bov_0.02_3m_2Pa
4	C_NI1_Bov_0.04_2m_
5	C_NI1_Bov_0.04_3m_
6	C_NI1_Bov_0.04_3m_2P
7	C_NI1_Bov_0.04_3m_2Pa
8	C_NI1_Bov_0.10_3m_
9	C_NI1_Bov_0.10_3m_2P
10	C_NI1_Bov_0.10_3m_2Pa
11	C_NI1_Bov_0.25_3m_
12	C_NI1_Bov_0.25_3m_2P
13	C_NI1_Bov_0.25_3m_2Pa
14	C_NI1_Bov_0.50_2m_
15	C_NI1_Bov_0.50_3m_
16	C_NI1_Bov_0.50_3m_2P
17	C_NI1_Bov_0.50_3m_2Pa
18	C_NI1_Bov_0.75_3m_
19	C_NI1_Bov_0.75_3m_2P
20	C_NI1_Bov_0.75_3m_2Pa
21	C_NI1_Bov_1.00_2m_
22	C_NI1_Bov_1.00_3m_
23	C_NI1_Bov_1.00_3m_2P
24	C_NI1_Bov_1.00_3m_2Pa
25	C_NI1_Bov_1.25_3m_
26	C_NI1_Bov_1.25_3m_2P
27	C_NI1_Bov_1.25_3m_2Pa
28	C_NI1_Bov_1.50_3m_
29	C_NI1_Bov_1.50_3m_2P
30	C_NI1_Bov_1.50_3m_2Pa
31	C_NI1_Bov_2.00_2m_
32	C_NI1_Bov_2.00_3m_
33	C_NI1_Bov_2.00_3m_2P
34	C_NI1_Bov_2.00_3m_2Pa
35	C_NI1_Bov_3.00_2m_
36	C_NI1_Bov_3.00_3m_
37	C_NI1_Bov_3.00_3m_2P
38	C_NI1_Bov_3.00_3m_2Pa
39	C_NI1_Bov_4.00_3m_
40	C_NI1_Bov_4.00_3m_2P
41	C_NI1_Bov_4.00_3m_2Pa
42	C_NI1_Bov_5.00_3m_
43	C_NI1_Bov_6.00_2m_

Number	OpenSees Run Name
44	C_NI1_Del_0.02_2m_
45	C_NI1_Del_0.02_3m_
46	C_NI1_Del_0.02_3m_2P
47	C_NI1_Del_0.02_3m_2Pa
48	C_NI1_Del_0.04_2m_
49	C_NI1_Del_0.04_3m_
50	C_NI1_Del_0.04_3m_2P
51	C_NI1_Del_0.04_3m_2Pa
52	C_NI1_Del_0.10_2m_
53	C_NI1_Del_0.10_3m_
54	C_NI1_Del_0.10_3m_2P
55	C_NI1_Del_0.10_3m_2Pa
56	C_NI1_Del_0.25_2m_
57	C_NI1_Del_0.25_3m_
58	C_NI1_Del_0.25_3m_2P
59	C_NI1_Del_0.25_3m_2Pa
60	C_NI1_Del_0.50_2m_
61	C_NI1_Del_0.50_3m_
62	C_NI1_Del_0.50_3m_2P
63	C_NI1_Del_0.50_3m_2Pa
64	C_NI1_Del_0.75_2m_
65	C_NI1_Del_0.75_3m_
66	C_NI1_Del_0.75_3m_2P
67	C_NI1_Del_0.75_3m_2Pa
68	C_NI1_Del_1.00_2m_
69	C_NI1_Del_1.00_3m_
70	C_NI1_Del_1.00_3m_2P
71	C_NI1_Del_1.00_3m_2Pa
72	C_NI1_Del_2.00_3m_
73	C_NI1_Elc_0.02_2m_
74	C_NI1_Elc_0.02_3m_
75	C_NI1_Elc_0.02_3m_2P
76	C_NI1_Elc_0.02_3m_2Pa
77	C_NI1_Elc_0.04_3m_
78	C_NI1_Elc_0.04_3m_2P
79	C_NI1_Elc_0.04_3m_2Pa
80	C_NI1_Elc_0.10_2m_
81	C_NI1_Elc_0.10_3m_
82	C_NI1_Elc_0.10_3m_2P
83	C_NI1_Elc_0.10_3m_2Pa
84	C_NI1_Elc_0.25_2m_
85	C_NI1_Elc_0.25_3m_
86	C_NI1_Elc_0.25_3m_2P

Number	OpenSees Run Name
87	C_NI1_Elc_0.25_3m_2Pa
88	C_NI1_Elc_0.40_3m_
89	C_NI1_Elc_0.40_3m_2P
90	C_NI1_Elc_0.40_3m_2Pa
91	C_NI1_Elc_0.50_2m_
92	C_NI1_Elc_0.50_3m_
93	C_NI1_Elc_0.50_3m_2P
94	C_NI1_Elc_0.50_3m_2Pa
95	C_NI1_Elc_0.75_2m_
96	C_NI1_Elc_0.75_3m_
97	C_NI1_Elc_0.75_3m_2P
98	C_NI1_Elc_0.75_3m_2Pa
99	C_NI1_Elc_1.00_2m_
100	C_NI1_Elc_1.00_3m_
101	C_NI1_Elc_1.00_3m_2P
102	C_NI1_Elc_1.00_3m_2Pa
103	C_NI1_Elc_1.25_3m_
104	C_NI1_Elc_1.50_3m_
105	C_NI1_Elc_2.00_3m_
106	C_NI1_Kal_0.02_3m_
107	C_NI1_Kal_0.02_3m_2P
108	C_NI1_Kal_0.02_3m_2Pa
109	C_NI1_Kal_0.04_3m_
110	C_NI1_Kal_0.04_3m_2P
111	C_NI1_Kal_0.04_3m_2Pa
112	C_NI1_Kal_0.10_2m_
113	C_NI1_Kal_0.10_3m_
114	C_NI1_Kal_0.10_3m_2P
115	C_NI1_Kal_0.10_3m_2Pa
116	C_NI1_Kal_0.25_3m_
117	C_NI1_Kal_0.25_3m_2P
118	C_NI1_Kal_0.25_3m_2Pa
119	C_NI1_Kal_0.50_2m_
120	C_NI1_Kal_0.50_3m_
121	C_NI1_Kal_0.50_3m_2P
122	C_NI1_Kal_0.50_3m_2Pa
123	C_NI1_Kal_0.75_3m_
124	C_NI1_Kal_0.75_3m_2P
125	C_NI1_Kal_0.75_3m_2Pa
126	C_NI1_Kal_1.00_2m_
127	C_NI1_Kal_1.00_3m_
128	C_NI1_Kal_1.00_3m_2P
129	C_NI1_Kal_1.00_3m_2Pa

Number	OpenSees Run Name
130	C_NI1_Kal_1.25_3m_
131	C_NI1_Kal_1.25_3m_2P
132	C_NI1_Kal_1.25_3m_2Pa
133	C_NI1_Kal_1.50_3m_
134	C_NI1_Kal_1.50_3m_2P
135	C_NI1_Kal_1.50_3m_2Pa
136	C_NI1_Kal_1.75_3m_
137	C_NI1_Kal_1.75_3m_2P
138	C_NI1_Kal_1.75_3m_2Pa
139	C_NI1_Kal_2.00_2m_
140	C_NI1_Kal_2.00_3m_
141	C_NI1_Kal_2.00_3m_2P
142	C_NI1_Kal_2.00_3m_2Pa
143	C_NI1_Kal_3.00_3m_
144	C_NI1_Kal_3.00_3m_2P
145	C_NI1_Kal_3.00_3m_2Pa
146	C_NI1_Kal_4.00_2m_
147	C_NI1_Kal_5.00_2m_
148	C_NI1_Mat_0.02_3m_
149	C_NI1_Mat_0.02_3m_2P
150	C_NI1_Mat_0.02_3m_2Pa
151	C_NI1_Mat_0.04_3m_
152	C_NI1_Mat_0.04_3m_2P
153	C_NI1_Mat_0.04_3m_2Pa
154	C_NI1_Mat_0.10_2m_
155	C_NI1_Mat_0.10_3m_
156	C_NI1_Mat_0.10_3m_2P
157	C_NI1_Mat_0.10_3m_2Pa
158	C_NI1_Mat_0.25_2m_
159	C_NI1_Mat_0.25_3m_
160	C_NI1_Mat_0.25_3m_2P
161	C_NI1_Mat_0.25_3m_2Pa
162	C_NI1_Mat_0.40_3m_
163	C_NI1_Mat_0.40_3m_2P
164	C_NI1_Mat_0.40_3m_2Pa
165	C_NI1_Mat_0.50_2m_
166	C_NI1_Mat_0.50_3m_
167	C_NI1_Mat_0.50_3m_2P
168	C_NI1_Mat_0.50_3m_2Pa
169	C_NI1_Mat_0.75_2m_
170	C_NI1_Mat_0.75_3m_
171	C_NI1_Mat_0.75_3m_2P
172	C_NI1_Mat_0.75_3m_2Pa

Number	OpenSees Run Name
173	C_NI1_Mat_1.00_2m_
174	C_NI1_Mat_1.00_3m_
175	C_NI1_Mat_1.00_3m_2P
176	C_NI1_Mat_1.00_3m_2Pa
177	C_NI1_Mat_1.25_2m_
178	C_NI1_Mat_1.25_3m_
179	C_NI1_Mat_2.00_3m_
180	C_NI2_Duz_0.02_2m_
181	C_NI2_Duz_0.02_3m_
182	C_NI2_Duz_0.02_3m_2P
183	C_NI2_Duz_0.02_3m_2Pa
184	C_NI2_Duz_0.04_3m_
185	C_NI2_Duz_0.04_3m_2P
186	C_NI2_Duz_0.04_3m_2Pa
187	C_NI2_Duz_0.10_2m_
188	C_NI2_Duz_0.10_3m_
189	C_NI2_Duz_0.10_3m_2P
190	C_NI2_Duz_0.10_3m_2Pa
191	C_NI2_Duz_0.15_3m_
192	C_NI2_Duz_0.15_3m_2P
193	C_NI2_Duz_0.15_3m_2Pa
194	C_NI2_Duz_0.25_2m_
195	C_NI2_Duz_0.25_3m_
196	C_NI2_Duz_0.25_3m_2P
197	C_NI2_Duz_0.25_3m_2Pa
198	C_NI2_Duz_0.35_3m_
199	C_NI2_Duz_0.35_3m_2P
200	C_NI2_Duz_0.35_3m_2Pa
201	C_NI2_Duz_0.50_2m_
202	C_NI2_Duz_0.50_3m_
203	C_NI2_Duz_0.50_3m_2P
204	C_NI2_Duz_0.50_3m_2Pa
205	C_NI2_Duz_0.75_2m_
206	C_NI2_Duz_0.75_3m_
207	C_NI2_Duz_0.75_3m_2P
208	C_NI2_Duz_0.75_3m_2Pa
209	C_NI2_Duz_1.00_2m_
210	C_NI2_Duz_1.00_3m_
211	C_NI2_Duz_1.00_3m_2P
212	C_NI2_Duz_1.00_3m_2Pa
213	C_NI2_Duz_2.00_3m_
214	C_NI2_Duz_2.00_3m_2P
215	C_NI2_Duz_2.00_3m_2Pa

Number	OpenSees Run Name
216	C_NI2_Koc_0.02_3m_
217	C_NI2_Koc_0.04_3m_
218	C_NI2_Koc_0.10_2m_
219	C_NI2_Koc_0.10_3m_
220	C_NI2_Koc_0.10_3m_2P
221	C_NI2_Koc_0.10_3m_2Pa
222	C_NI2_Koc_0.25_3m_
223	C_NI2_Koc_0.25_3m_2P
224	C_NI2_Koc_0.25_3m_2Pa
225	C_NI2_Koc_0.50_2m_
226	C_NI2_Koc_0.50_3m_
227	C_NI2_Koc_0.50_3m_2P
228	C_NI2_Koc_0.50_3m_2Pa
229	C_NI2_Koc_0.75_3m_
230	C_NI2_Koc_0.75_3m_2P
231	C_NI2_Koc_0.75_3m_2Pa
232	C_NI2_Koc_1.00_2m_
233	C_NI2_Koc_1.00_3m_
234	C_NI2_Koc_1.00_3m_2P
235	C_NI2_Koc_1.00_3m_2Pa
236	C_NI2_Koc_1.25_3m_
237	C_NI2_Koc_1.25_3m_2P
238	C_NI2_Koc_1.25_3m_2Pa
239	C_NI2_Koc_1.50_3m_
240	C_NI2_Koc_1.50_3m_2P
241	C_NI2_Koc_1.50_3m_2Pa
242	C_NI2_Koc_2.00_2m_
243	C_NI2_Koc_2.00_3m_
244	C_NI2_Koc_2.00_3m_2P
245	C_NI2_Koc_2.00_3m_2Pa
246	C_NI2_Koc_3.00_3m_
247	C_NI2_Koc_4.00_2m_
248	C_NI2_Koc_6.00_2m_
249	C_NI2_Lau_0.02_2m_
250	C_NI2_Lau_0.02_3m_
251	C_NI2_Lau_0.02_3m_2P
252	C_NI2_Lau_0.02_3m_2Pa
253	C_NI2_Lau_0.04_3m_
254	C_NI2_Lau_0.04_3m_2P
255	C_NI2_Lau_0.04_3m_2Pa
256	C_NI2_Lau_0.10_2m_
257	C_NI2_Lau_0.10_3m_
258	C_NI2_Lau_0.10_3m_2P

Number	OpenSees Run Name
259	C_NI2_Lau_0.10_3m_2Pa
260	C_NI2_Lau_0.25_3m_
261	C_NI2_Lau_0.25_3m_2P
262	C_NI2_Lau_0.25_3m_2Pa
263	C_NI2_Lau_0.50_3m_
264	C_NI2_Lau_0.50_3m_2P
265	C_NI2_Lau_0.50_3m_2Pa
266	C_NI2_Lau_0.75_3m_
267	C_NI2_Lau_0.75_3m_2P
268	C_NI2_Lau_0.75_3m_2Pa
269	C_NI2_Lau_1.00_2m_
270	C_NI2_Lau_1.00_3m_
271	C_NI2_Lau_1.00_3m_2P
272	C_NI2_Lau_1.00_3m_2Pa
273	C_NI2_Lau_1.25_3m_
274	C_NI2_Lau_1.25_3m_2P
275	C_NI2_Lau_1.25_3m_2Pa
276	C_NI2_Lau_1.50_2m_
277	C_NI2_Lau_1.50_3m_
278	C_NI2_Lau_1.50_3m_2P
279	C_NI2_Lau_1.50_3m_2Pa
280	C_NI2_Lau_1.75_3m_
281	C_NI2_Lau_1.75_3m_2P
282	C_NI2_Lau_1.75_3m_2Pa
283	C_NI2_Lau_2.00_2m_
284	C_NI2_Lau_2.00_3m_
285	C_NI2_Lau_2.00_3m_2P
286	C_NI2_Lau_2.00_3m_2Pa
287	C_NI2_Luc_0.02_2m_
288	C_NI2_Luc_0.02_3m_
289	C_NI2_Luc_0.02_3m_2P
290	C_NI2_Luc_0.02_3m_2Pa
291	C_NI2_Luc_0.04_3m_
292	C_NI2_Luc_0.04_3m_2P
293	C_NI2_Luc_0.04_3m_2Pa
294	C_NI2_Luc_0.10_2m_
295	C_NI2_Luc_0.10_3m_
296	C_NI2_Luc_0.10_3m_2P
297	C_NI2_Luc_0.10_3m_2Pa
298	C_NI2_Luc_0.25_2m_
299	C_NI2_Luc_0.25_3m_
300	C_NI2_Luc_0.25_3m_2P
301	C_NI2_Luc_0.25_3m_2Pa

Number	OpenSees Run Name
302	C_NI2_Luc_0.40_3m_
303	C_NI2_Luc_0.40_3m_2P
304	C_NI2_Luc_0.40_3m_2Pa
305	C_NI2_Luc_0.50_2m_
306	C_NI2_Luc_0.50_3m_
307	C_NI2_Luc_0.50_3m_2P
308	C_NI2_Luc_0.50_3m_2Pa
309	C_NI2_Luc_0.75_2m_
310	C_NI2_Luc_0.75_3m_
311	C_NI2_Luc_0.75_3m_2P
312	C_NI2_Luc_0.75_3m_2Pa
313	C_NI2_Luc_1.00_2m_
314	C_NI2_Luc_1.00_3m_
315	C_NI2_Luc_1.00_3m_2P
316	C_NI2_Luc_1.00_3m_2Pa
317	C_NI2_Luc_2.00_3m_
318	C_NI2_Tab_0.01_2m_
319	C_NI2_Tab_0.01_3m_
320	C_NI2_Tab_0.01_3m_2P
321	C_NI2_Tab_0.01_3m_2Pa
322	C_NI2_Tab_0.02_3m_
323	C_NI2_Tab_0.02_3m_2P
324	C_NI2_Tab_0.02_3m_2Pa
325	C_NI2_Tab_0.04_2m_
326	C_NI2_Tab_0.04_3m_
327	C_NI2_Tab_0.04_3m_2P
328	C_NI2_Tab_0.06_3m_
329	C_NI2_Tab_0.06_3m_2P
330	C_NI2_Tab_0.06_3m_2Pa
331	C_NI2_Tab_0.10_2m_
332	C_NI2_Tab_0.10_3m_
333	C_NI2_Tab_0.10_3m_2P
334	C_NI2_Tab_0.10_3m_2Pa
335	C_NI2_Tab_0.12_3m_
336	C_NI2_Tab_0.12_3m_2P
337	C_NI2_Tab_0.12_3m_2Pa
338	C_NI2_Tab_0.15_2m_
339	C_NI2_Tab_0.15_3m_
340	C_NI2_Tab_0.15_3m_2P
341	C_NI2_Tab_0.15_3m_2Pa
342	C_NI2_Tab_0.25_2m_
343	C_NI2_Tab_0.25_3m_
344	C_NI2_Tab_0.25_3m_2P

Number	OpenSees Run Name
345	C_NI2_Tab_0.25_3m_2Pa
346	C_NI2_Tab_0.35_3m_
347	C_NI2_Tab_0.35_3m_2P
348	C_NI2_Tab_0.35_3m_2Pa
349	C_NI2_Tab_0.50_3m_
350	C_SI1_Chi_0.02_2m_
351	C_SI1_Chi_0.02_3m_
352	C_SI1_Chi_0.02_3m_2P
353	C_SI1_Chi_0.02_3m_2Pa
354	C_SI1_Chi_0.04_2m_
355	C_SI1_Chi_0.04_3m_
356	C_SI1_Chi_0.04_3m_2P
357	C_SI1_Chi_0.04_3m_2Pa
358	C_SI1_Chi_0.10_2m_
359	C_SI1_Chi_0.10_3m_
360	C_SI1_Chi_0.10_3m_2P
361	C_SI1_Chi_0.10_3m_2Pa
362	C_SI1_Chi_0.25_2m_
363	C_SI1_Chi_0.25_3m_
364	C_SI1_Chi_0.25_3m_2P
365	C_SI1_Chi_0.25_3m_2Pa
366	C_SI1_Chi_0.50_2m_
367	C_SI1_Chi_0.50_3m_
368	C_SI1_Chi_0.50_3m_2P
369	C_SI1_Chi_0.50_3m_2Pa
370	C_SI1_Chi_0.75_2m_
371	C_SI1_Chi_0.75_3m_
372	C_SI1_Chi_0.75_3m_2P
373	C_SI1_Chi_0.75_3m_2Pa
374	C_SI1_Chi_1.00_2m_
375	C_SI1_Chi_1.00_3m_
376	C_SI1_Chi_1.00_3m_2P
377	C_SI1_Chi_1.00_3m_2Pa
378	C_SI1_Chi_1.25_3m_
379	C_SI1_Chi_1.25_3m_2P
380	C_SI1_Chi_1.25_3m_2Pa
381	C_SI1_Chi_1.50_2m_
382	C_SI1_Chi_1.50_3m_
383	C_SI1_Chi_1.50_3m_2P
384	C_SI1_Chi_1.50_3m_2Pa
385	C_SI1_Chi_1.75_2m_
386	C_SI1_Chi_1.75_3m_
387	C_SI1_Chi_1.75_3m_2P

Number	OpenSees Run Name
388	C_SI1_Chi_1.75_3m_2Pa
389	C_SI1_Chi_2.00_3m_
390	C_SI1_Hec_0.02_3m_
391	C_SI1_Hec_0.02_3m_2P
392	C_SI1_Hec_0.02_3m_2Pa
393	C_SI1_Hec_0.04_3m_
394	C_SI1_Hec_0.04_3m_2P
395	C_SI1_Hec_0.04_3m_2Pa
396	C_SI1_Hec_0.10_2m_
397	C_SI1_Hec_0.10_3m_
398	C_SI1_Hec_0.10_3m_2P
399	C_SI1_Hec_0.10_3m_2Pa
400	C_SI1_Hec_0.25_3m_
401	C_SI1_Hec_0.25_3m_2P
402	C_SI1_Hec_0.25_3m_2Pa
403	C_SI1_Hec_0.50_2m_
404	C_SI1_Hec_0.50_3m_
405	C_SI1_Hec_0.50_3m_2P
406	C_SI1_Hec_0.50_3m_2Pa
407	C_SI1_Hec_0.75_3m_
408	C_SI1_Hec_0.75_3m_2P
409	C_SI1_Hec_0.75_3m_2Pa
410	C_SI1_Hec_1.00_2m_
411	C_SI1_Hec_1.00_3m_
412	C_SI1_Hec_1.00_3m_2P
413	C_SI1_Hec_1.00_3m_2Pa
414	C_SI1_Hec_1.50_3m_
415	C_SI1_Hec_1.50_3m_2P
416	C_SI1_Hec_1.50_3m_2Pa
417	C_SI1_Hec_2.00_2m_
418	C_SI1_Hec_2.00_3m_
419	C_SI1_Hec_2.00_3m_2P
420	C_SI1_Hec_2.00_3m_2Pa
421	C_SI1_Hec_3.00_3m_
422	C_SI1_Hec_3.00_3m_2P
423	C_SI1_Hec_3.00_3m_2Pa
424	C_SI1_Hec_4.00_2m_
425	C_SI1_Hec_4.00_3m_
426	C_SI1_Hec_4.00_3m_2P
427	C_SI1_Hec_4.00_3m_2Pa
428	C_SI1_Hec_6.00_2m_
429	C_SI1_Koc_0.02_2m_
430	C_SI1_Koc_0.02_3m_

Number	OpenSees Run Name
431	C_SI1_Koc_0.02_3m_2P
432	C_SI1_Koc_0.02_3m_2Pa
433	C_SI1_Koc_0.04_2m_
434	C_SI1_Koc_0.04_3m_
435	C_SI1_Koc_0.04_3m_2P
436	C_SI1_Koc_0.04_3m_2Pa
437	C_SI1_Koc_0.10_2m_
438	C_SI1_Koc_0.10_3m_
439	C_SI1_Koc_0.10_3m_2P
440	C_SI1_Koc_0.10_3m_2Pa
441	C_SI1_Koc_0.25_2m_
442	C_SI1_Koc_0.25_3m_
443	C_SI1_Koc_0.25_3m_2P
444	C_SI1_Koc_0.25_3m_2Pa
445	C_SI1_Koc_0.50_2m_
446	C_SI1_Koc_0.50_3m_
447	C_SI1_Koc_0.50_3m_2P
448	C_SI1_Koc_0.50_3m_2Pa
449	C_SI1_Koc_0.75_3m_
450	C_SI1_Koc_0.75_3m_2P
451	C_SI1_Koc_0.75_3m_2Pa
452	C_SI1_Koc_1.00_2m_
453	C_SI1_Koc_1.00_3m_
454	C_SI1_Koc_1.00_3m_2P
455	C_SI1_Koc_1.00_3m_2Pa
456	C_SI1_Koc_1.25_3m_
457	C_SI1_Koc_1.25_3m_2P
458	C_SI1_Koc_1.25_3m_2Pa
459	C_SI1_Lan_0.02_2m_
460	C_SI1_Lan_0.02_3m_
461	C_SI1_Lan_0.02_3m_2P
462	C_SI1_Lan_0.02_3m_2Pa
463	C_SI1_Lan_0.04_3m_
464	C_SI1_Lan_0.04_3m_2P
465	C_SI1_Lan_0.04_3m_2Pa
466	C_SI1_Lan_0.10_2m_
467	C_SI1_Lan_0.10_3m_
468	C_SI1_Lan_0.10_3m_2P
469	C_SI1_Lan_0.10_3m_2Pa
470	C_SI1_Lan_0.25_3m_
471	C_SI1_Lan_0.25_3m_2P
472	C_SI1_Lan_0.25_3m_2Pa
473	C_SI1_Lan_0.50_2m_

Number	OpenSees Run Name
474	C_SI1_Lan_0.50_3m_
475	C_SI1_Lan_0.50_3m_2P
476	C_SI1_Lan_0.50_3m_2Pa
477	C_SI1_Lan_0.75_3m_
478	C_SI1_Lan_0.75_3m_2P
479	C_SI1_Lan_0.75_3m_2Pa
480	C_SI1_Lan_1.00_2m_
481	C_SI1_Lan_1.00_3m_
482	C_SI1_Lan_1.00_3m_2P
483	C_SI1_Lan_1.00_3m_2Pa
484	C_SI1_Lan_1.50_2m_
485	C_SI1_Lan_1.50_3m_
486	C_SI1_Lan_1.50_3m_2P
487	C_SI1_Lan_1.50_3m_2Pa
488	C_SI1_Lan_2.00_3m_
489	C_SI1_Lan_2.00_3m_2P
490	C_SI1_Lan_2.00_3m_2Pa
491	C_SI1_Lan_2.50_2m_
492	C_SI1_Lan_2.50_3m_
493	C_SI1_Lan_2.50_3m_2P
494	C_SI1_Lan_2.50_3m_2Pa
495	C_SI1_Nor_0.02_2m_
496	C_SI1_Nor_0.02_3m_
497	C_SI1_Nor_0.02_3m_2P
498	C_SI1_Nor_0.02_3m_2Pa
499	C_SI1_Nor_0.04_3m_
500	C_SI1_Nor_0.04_3m_2P
501	C_SI1_Nor_0.04_3m_2Pa
502	C_SI1_Nor_0.10_2m_
503	C_SI1_Nor_0.10_3m_
504	C_SI1_Nor_0.10_3m_2P
505	C_SI1_Nor_0.10_3m_2Pa
506	C_SI1_Nor_0.25_3m_
507	C_SI1_Nor_0.25_3m_2P
508	C_SI1_Nor_0.25_3m_2Pa
509	C_SI1_Nor_0.50_2m_
510	C_SI1_Nor_0.50_3m_
511	C_SI1_Nor_0.50_3m_2P
512	C_SI1_Nor_0.50_3m_2Pa
513	C_SI1_Nor_0.75_3m_
514	C_SI1_Nor_0.75_3m_2P
515	C_SI1_Nor_0.75_3m_2Pa
516	C_SI1_Nor_1.00_2m_

Number	OpenSees Run Name	Number	OpenSees Run Name
474	C_SI1_Lan_0.50_3m_	517	C_SI1_Nor_1.00_3m_
475	C_SI1_Lan_0.50_3m_2P	518	C_SI1_Nor_1.00_3m_2P
476	C_SI1_Lan_0.50_3m_2Pa	519	C_SI1_Nor_1.00_3m_2Pa
477	C_SI1_Lan_0.75_3m_	520	C_SI1_Nor_1.50_3m_
478	C_SI1_Lan_0.75_3m_2P	521	C_SI1_Nor_1.50_3m_2P
479	C_SI1_Lan_0.75_3m_2Pa	522	C_SI1_Nor_1.50_3m_2Pa
480	C_SI1_Lan_1.00_2m_	523	C_SI1_Nor_2.00_2m_
481	C_SI1_Lan_1.00_3m_	524	C_SI1_Nor_2.00_3m_
482	C_SI1_Lan_1.00_3m_2P	525	C_SI1_Nor_2.00_3m_2P
483	C_SI1_Lan_1.00_3m_2Pa	526	C_SI1_Nor_2.00_3m_2Pa
484	C_SI1_Lan_1.50_2m_	527	C_SI1_Nor_3.00_3m_
485	C_SI1_Lan_1.50_3m_	528	C_SI1_Nor_3.00_3m_2P
486	C_SI1_Lan_1.50_3m_2P	529	C_SI1_Nor_3.00_3m_2Pa
487	C_SI1_Lan_1.50_3m_2Pa	530	C_SI1_Nor_4.00_2m_
488	C_SI1_Lan_2.00_3m_	531	C_SI1_Nor_4.00_3m_
489	C_SI1_Lan_2.00_3m_2P	532	C_SI1_Nor_4.00_3m_2P
490	C_SI1_Lan_2.00_3m_2Pa	533	C_SI1_Nor_4.00_3m_2Pa
491	C_SI1_Lan_2.50_2m_	534	C_SI1_Nor_6.00_2m_
492	C_SI1_Lan_2.50_3m_	535	C_SI1_San_0.02_2m_
493	C_SI1_Lan_2.50_3m_2P	536	C_SI1_San_0.02_3m_
494	C_SI1_Lan_2.50_3m_2Pa	537	C_SI1_San_0.02_3m_2P
495	C_SI1_Nor_0.02_2m_	538	C_SI1_San_0.02_3m_2Pa
496	C_SI1_Nor_0.02_3m_	539	C_SI1_San_0.04_3m_
497	C_SI1_Nor_0.02_3m_2P	540	C_SI1_San_0.04_3m_2P
498	C_SI1_Nor_0.02_3m_2Pa	541	C_SI1_San_0.04_3m_2Pa
499	C_SI1_Nor_0.04_3m_	542	C_SI1_San_0.10_2m_
500	C_SI1_Nor_0.04_3m_2P	543	C_SI1_San_0.10_3m_
501	C_SI1_Nor_0.04_3m_2Pa	544	C_SI1_San_0.10_3m_2P
502	C_SI1_Nor_0.10_2m_	545	C_SI1_San_0.10_3m_2Pa
503	C_SI1_Nor_0.10_3m_	546	C_SI1_San_0.25_3m_
504	C_SI1_Nor_0.10_3m_2P	547	C_SI1_San_0.25_3m_2P
505	C_SI1_Nor_0.10_3m_2Pa	548	C_SI1_San_0.25_3m_2Pa
506	C_SI1_Nor_0.25_3m_	549	C_SI1_San_0.50_2m_
507	C_SI1_Nor_0.25_3m_2P	550	C_SI1_San_0.50_3m_
508	C_SI1_Nor_0.25_3m_2Pa	551	C_SI1_San_0.50_3m_2P
509	C_SI1_Nor_0.50_2m_	552	C_SI1_San_0.50_3m_2Pa
510	C_SI1_Nor_0.50_3m_	553	C_SI1_San_0.75_3m_
511	C_SI1_Nor_0.50_3m_2P	554	C_SI1_San_0.75_3m_2P
512	C_SI1_Nor_0.50_3m_2Pa	555	C_SI1_San_0.75_3m_2Pa
513	C_SI1_Nor_0.75_3m_	556	C_SI1_San_1.00_2m_
514	C_SI1_Nor_0.75_3m_2P	557	C_SI1_San_1.00_3m_
515	C_SI1_Nor_0.75_3m_2Pa	558	C_SI1_San_1.00_3m_2P
516	C_SI1_Nor_1.00_2m_	559	C_SI1_San_1.00_3m_2Pa

Number	OpenSees Run Name
560	C_SI1_San_1.50_3m_
561	C_SI1_San_1.50_3m_2P
562	C_SI1_San_1.50_3m_2Pa
563	C_SI1_San_2.00_2m_
564	C_SI1_San_2.00_3m_
565	C_SI1_San_2.00_3m_2P
566	C_SI1_San_2.00_3m_2Pa
567	C_SI1_San_3.00_2m_
568	C_SI1_San_3.00_3m_
569	C_SI1_San_3.00_3m_2P
570	C_SI1_San_3.00_3m_2Pa
571	C_SI1_San_4.00_2m_
572	D_NI1_Cor_0.02_2m_
573	D_NI1_Cor_0.02_3m_
574	D_NI1_Cor_0.02_3m_2P
575	D_NI1_Cor_0.02_3m_2Pa
576	D_NI1_Cor_0.10_2m_
577	D_NI1_Cor_0.10_3m_
578	D_NI1_Cor_0.10_3m_2P
579	D_NI1_Cor_0.10_3m_2Pa
580	D_NI1_Cor_0.25_2m_
581	D_NI1_Cor_0.25_3m_
582	D_NI1_Cor_0.25_3m_2P
583	D_NI1_Cor_0.25_3m_2Pa
584	D_NI1_Cor_0.50_2m_
585	D_NI1_Cor_0.50_3m_
586	D_NI1_Cor_0.50_3m_2P
587	D_NI1_Cor_0.50_3m_2Pa
588	D_NI1_Cor_0.75_2m_
589	D_NI1_Cor_0.75_3m_
590	D_NI1_Cor_0.75_3m_2P
591	D_NI1_Cor_0.75_3m_2Pa
592	D_NI1_Cor_1.00_2m_
593	D_NI1_Cor_1.00_3m_
594	D_NI1_Cor_1.00_3m_2P
595	D_NI1_Cor_1.00_3m_2Pa
596	D_NI1_Del_0.02_2m_
597	D_NI1_Del_0.02_3m_
598	D_NI1_Del_0.02_3m_2P
599	D_NI1_Del_0.02_3m_2Pa
600	D_NI1_Del_0.10_2m_
601	D_NI1_Del_0.10_3m_
602	D_NI1_Del_0.10_3m_2P

Number	OpenSees Run Name
603	D_NI1_Del_0.10_3m_2Pa
604	D_NI1_Del_0.25_2m_
605	D_NI1_Del_0.25_3m_
606	D_NI1_Del_0.25_3m_2P
607	D_NI1_Del_0.25_3m_2Pa
608	D_NI1_Del_0.50_2m_
609	D_NI1_Del_0.50_3m_
610	D_NI1_Del_0.50_3m_2P
611	D_NI1_Del_0.50_3m_2Pa
612	D_NI1_Del_0.75_2m_
613	D_NI1_Del_0.75_3m_
614	D_NI1_Del_0.75_3m_2P
615	D_NI1_Del_0.75_3m_2Pa
616	D_NI1_Del_1.00_2m_
617	D_NI1_Del_1.00_3m_
618	D_NI1_Del_1.00_3m_2P
619	D_NI1_Del_1.00_3m_2Pa
620	D_NI1_Elc_0.02_2m_
621	D_NI1_Elc_0.02_3m_
622	D_NI1_Elc_0.02_3m_2P
623	D_NI1_Elc_0.02_3m_2Pa
624	D_NI1_Elc_0.10_2m_
625	D_NI1_Elc_0.10_3m_
626	D_NI1_Elc_0.10_3m_2P
627	D_NI1_Elc_0.10_3m_2Pa
628	D_NI1_Elc_0.25_2m_
629	D_NI1_Elc_0.25_3m_
630	D_NI1_Elc_0.25_3m_2P
631	D_NI1_Elc_0.25_3m_2Pa
632	D_NI1_Elc_0.35_2m_
633	D_NI1_Elc_0.50_2m_
634	D_NI1_Elc_0.50_3m_
635	D_NI1_Elc_0.50_3m_2P
636	D_NI1_Elc_0.50_3m_2Pa
637	D_NI1_Elc_0.75_3m_
638	D_NI1_Elc_0.75_3m_2P
639	D_NI1_Elc_0.75_3m_2Pa
640	D_NI1_Elc_1.00_2m_
641	D_NI1_Elc_1.00_3m_
642	D_NI1_Elc_1.00_3m_2P
643	D_NI1_Elc_1.00_3m_2Pa
644	D_NI1_Elc_1.25_3m_
645	D_NI1_Elc_1.25_3m_2P

Number	OpenSees Run Name
646	D_NI1_Elc_1.25_3m_2Pa
647	D_NI1_Kal_0.02_2m_
648	D_NI1_Kal_0.02_3m_
649	D_NI1_Kal_0.04_3m_2P
650	D_NI1_Kal_0.04_3m_2Pa
651	D_NI1_Kal_0.10_2m_
652	D_NI1_Kal_0.10_3m_
653	D_NI1_Kal_0.25_2m_
654	D_NI1_Kal_0.25_3m_
655	D_NI1_Kal_0.50_2m_
656	D_NI1_Kal_0.50_3m_
657	D_NI1_Kal_0.50_3m_2P
658	D_NI1_Kal_0.50_3m_2Pa
659	D_NI1_Kal_1.00_2m_
660	D_NI1_Kal_1.00_3m_
661	D_NI1_Kal_1.00_3m_2P
662	D_NI1_Kal_1.00_3m_2Pa
663	D_NI1_Kal_1.50_3m_
664	D_NI1_Kal_1.50_3m_2P
665	D_NI1_Kal_1.50_3m_2Pa
666	D_NI1_Kal_2.00_2m_
667	D_NI1_Kal_2.00_3m_2P
668	D_NI1_Kal_2.00_3m_2Pa
669	D_NI1_Kal_2.50_3m_2P
670	D_NI1_Kal_2.50_3m_2Pa
671	D_NI1_Kal_3.00_3m_2P
672	D_NI1_Kal_3.00_3m_2Pa
673	D_NI1_Wes_0.02_2m_
674	D_NI1_Wes_0.02_3m_
675	D_NI1_Wes_0.02_3m_2P
676	D_NI1_Wes_0.02_3m_2Pa
677	D_NI1_Wes_0.10_2m_
678	D_NI1_Wes_0.10_3m_2P
679	D_NI1_Wes_0.10_3m_2Pa
680	D_NI1_Wes_0.25_2m_
681	D_NI1_Wes_0.25_3m_
682	D_NI1_Wes_0.25_3m_2P
683	D_NI1_Wes_0.25_3m_2Pa
684	D_NI1_Wes_0.50_2m_
685	D_NI1_Wes_0.50_3m_
686	D_NI1_Wes_0.50_3m_2P
687	D_NI1_Wes_0.50_3m_2Pa
688	D_NI1_Wes_0.75_2m_

Number	OpenSees Run Name
689	D_NI1_Wes_0.75_3m_
690	D_NI1_Wes_0.75_3m_2P
691	D_NI1_Wes_0.75_3m_2Pa
692	D_NI1_Wes_1.00_2m_
693	D_NI1_Wes_1.00_3m_
694	D_NI1_Wes_1.00_3m_2P
695	D_NI1_Wes_1.00_3m_2Pa
696	D_NI1_Wes_1.25_3m_
697	D_NI1_Wes_1.50_3m_
698	D_NI2_Cal_0.02_3m_2P
699	D_NI2_Cal_0.02_3m_2Pa
700	D_NI2_Cal_0.04_3m_
701	D_NI2_Cal_0.10_3m_
702	D_NI2_Cal_0.25_3m_
703	D_NI2_Cal_0.25_3m_2P
704	D_NI2_Cal_0.25_3m_2Pa
705	D_NI2_Cal_0.50_3m_
706	D_NI2_Cal_0.50_3m_2P
707	D_NI2_Cal_0.50_3m_2Pa
708	D_NI2_Cal_0.75_3m_
709	D_NI2_Cal_0.75_3m_2P
710	D_NI2_Cal_0.75_3m_2Pa
711	D_NI2_Cal_1.00_3m_
712	D_NI2_Cal_1.00_3m_2P
713	D_NI2_Cal_1.00_3m_2Pa
714	D_NI2_Cal_1.50_3m_
715	D_NI2_Cal_1.50_3m_2P
716	D_NI2_Cal_1.50_3m_2Pa
717	D_NI2_Cal_2.00_3m_2P
718	D_NI2_Cal_2.00_3m_2Pa
719	D_NI2_Duz_0.02_2m_
720	D_NI2_Duz_0.02_3m_
721	D_NI2_Duz_0.02_3m_2P
722	D_NI2_Duz_0.02_3m_2Pa
723	D_NI2_Duz_0.05_3m_
724	D_NI2_Duz_0.10_2m_
725	D_NI2_Duz_0.10_3m_
726	D_NI2_Duz_0.10_3m_2P
727	D_NI2_Duz_0.10_3m_2Pa
728	D_NI2_Duz_0.25_2m_
729	D_NI2_Duz_0.25_3m_
730	D_NI2_Duz_0.25_3m_2P
731	D_NI2_Duz_0.25_3m_2Pa

Number	OpenSees Run Name
732	D_NI2_Duz_0.35_3m_2P
733	D_NI2_Duz_0.35_3m_2Pa
734	D_NI2_Duz_0.50_2m_
735	D_NI2_Duz_0.50_3m_
736	D_NI2_Duz_0.50_3m_2P
737	D_NI2_Duz_0.50_3m_2Pa
738	D_NI2_Duz_0.75_2m_
739	D_NI2_Duz_0.75_3m_
740	D_NI2_Duz_0.75_3m_2P
741	D_NI2_Duz_0.75_3m_2Pa
742	D_NI2_Duz_1.00_2m_
743	D_NI2_Duz_1.00_3m_
744	D_NI2_Duz_1.00_3m_2P
745	D_NI2_Duz_1.00_3m_2Pa
746	D_NI2_Duz_1.25_2m_
747	D_NI2_Duz_1.25_3m_
748	D_NI2_El6_0.02_2m_
749	D_NI2_El6_0.02_3m_
750	D_NI2_El6_0.02_3m_2P
751	D_NI2_El6_0.02_3m_2Pa
752	D_NI2_El6_0.04_2m_
753	D_NI2_El6_0.04_3m_
754	D_NI2_El6_0.04_3m_2P
755	D_NI2_El6_0.04_3m_2Pa
756	D_NI2_El6_0.10_2m_
757	D_NI2_El6_0.10_3m_
758	D_NI2_El6_0.10_3m_2P
759	D_NI2_El6_0.10_3m_2Pa
760	D_NI2_El6_0.15_2m_
761	D_NI2_El6_0.15_3m_
762	D_NI2_El6_0.15_3m_2P
763	D_NI2_El6_0.15_3m_2Pa
764	D_NI2_El6_0.25_2m_
765	D_NI2_El6_0.25_3m_
766	D_NI2_El6_0.25_3m_2P
767	D_NI2_El6_0.25_3m_2Pa
768	D_NI2_El6_0.35_3m_
769	D_NI2_El6_0.35_3m_2P
770	D_NI2_El6_0.35_3m_2Pa
771	D_NI2_El6_0.50_2m_
772	D_NI2_El6_0.50_3m_
773	D_NI2_El6_0.50_3m_2P
774	D_NI2_El6_0.50_3m_2Pa

Number	OpenSees Run Name
775	D_NI2_El6_1.00_2m_
776	D_NI2_El6_1.00_3m_
777	D_NI2_El6_1.00_3m_2P
778	D_NI2_El6_1.00_3m_2Pa
779	D_NI2_Yar_0.02_3m_
780	D_NI2_Yar_0.02_3m_2P
781	D_NI2_Yar_0.04_3m_2P
782	D_NI2_Yar_0.04_3m_2Pa
783	D_NI2_Yar_0.10_3m_2P
784	D_NI2_Yar_0.10_3m_2Pa
785	D_NI2_Yar_0.25_2m_
786	D_NI2_Yar_0.25_3m_
787	D_NI2_Yar_0.25_3m_2P
788	D_NI2_Yar_0.25_3m_2Pa
789	D_NI2_Yar_0.35_2m_
790	D_NI2_Yar_0.35_3m_
791	D_NI2_Yar_0.35_3m_2P
792	D_NI2_Yar_0.35_3m_2Pa
793	D_NI2_Yar_0.50_3m_
794	D_NI2_Yar_0.50_3m_2P
795	D_NI2_Yar_0.50_3m_2Pa
796	D_NI2_Yar_0.75_3m_
797	D_NI2_Yar_0.75_3m_2P
798	D_NI2_Yar_0.75_3m_2Pa
799	D_NI2_Yar_1.00_2m_
800	D_NI2_Yar_1.00_3m_
801	D_NI2_Yar_1.00_3m_2P
802	D_NI2_Yar_1.00_3m_2Pa
803	D_SI1_Chi_0.02_2m_
804	D_SI1_Chi_0.02_3m_
805	D_SI1_Chi_0.02_3m_2P
806	D_SI1_Chi_0.02_3m_2Pa
807	D_SI1_Chi_0.10_2m_
808	D_SI1_Chi_0.10_3m_
809	D_SI1_Chi_0.25_2m_
810	D_SI1_Chi_0.25_3m_
811	D_SI1_Chi_0.25_3m_2P
812	D_SI1_Chi_0.25_3m_2Pa
813	D_SI1_Chi_0.50_2m_
814	D_SI1_Chi_0.50_3m_
815	D_SI1_Chi_0.50_3m_2P
816	D_SI1_Chi_0.50_3m_2Pa
817	D_SI1_Chi_1.00_2m_

Number	OpenSees Run Name
818	D_SI1_Chi_1.00_3m_
819	D_SI1_Chi_1.00_3m_2P
820	D_SI1_Chi_1.00_3m_2Pa
821	D_SI1_Chi_1.25_3m_
822	D_SI1_Chi_1.50_2m_
823	D_SI1_Chi_1.50_3m_2P
824	D_SI1_Chi_1.50_3m_2Pa
825	D_SI1_Chi_2.00_3m_2P
826	D_SI1_Chi_2.00_3m_2Pa
827	D_SI1_Hec_0.04_3m_
828	D_SI1_Hec_0.04_3m_2P
829	D_SI1_Hec_0.04_3m_2Pa
830	D_SI1_Hec_0.10_2m_
831	D_SI1_Hec_0.10_3m_
832	D_SI1_Hec_0.25_3m_
833	D_SI1_Hec_0.25_3m_2P
834	D_SI1_Hec_0.25_3m_2Pa
835	D_SI1_Hec_0.50_2m_
836	D_SI1_Hec_0.50_3m_
837	D_SI1_Hec_0.50_3m_2P
838	D_SI1_Hec_0.50_3m_2Pa
839	D_SI1_Hec_0.75_3m_
840	D_SI1_Hec_1.00_2m_
841	D_SI1_Hec_1.00_3m_
842	D_SI1_Hec_1.00_3m_2P
843	D_SI1_Hec_1.00_3m_2Pa
844	D_SI1_Hec_2.00_2m_
845	D_SI1_Hec_2.00_3m_2P
846	D_SI1_Hec_2.00_3m_2Pa
847	D_SI1_Hec_3.00_2m_
848	D_SI1_Hec_3.00_3m_2P
849	D_SI1_Hec_3.00_3m_2Pa
850	D_SI1_Hec_4.00_2m_
851	D_SI1_Koc_0.02_2m_
852	D_SI1_Koc_0.02_3m_
853	D_SI1_Koc_0.02_3m_2P
854	D_SI1_Koc_0.02_3m_2Pa
855	D_SI1_Koc_0.04_2m_
856	D_SI1_Koc_0.04_3m_2P
857	D_SI1_Koc_0.04_3m_2Pa
858	D_SI1_Koc_0.10_2m_
859	D_SI1_Koc_0.10_3m_
860	D_SI1_Koc_0.10_3m_2P

Number	OpenSees Run Name
861	D_SI1_Koc_0.10_3m_2Pa
862	D_SI1_Koc_0.25_2m_
863	D_SI1_Koc_0.25_3m_
864	D_SI1_Koc_0.25_3m_2P
865	D_SI1_Koc_0.25_3m_2Pa
866	D_SI1_Koc_0.50_2m_
867	D_SI1_Koc_0.50_3m_
868	D_SI1_Koc_0.50_3m_2P
869	D_SI1_Koc_0.50_3m_2Pa
870	D_SI1_Koc_0.75_3m_
871	D_SI1_Koc_1.00_2m_
872	D_SI1_Koc_1.00_3m_
873	D_SI1_Koc_1.00_3m_2P
874	D_SI1_Koc_1.00_3m_2Pa
875	D_SI1_Lan_0.02_2m_
876	D_SI1_Lan_0.02_3m_
877	D_SI1_Lan_0.02_3m_2P
878	D_SI1_Lan_0.02_3m_2Pa
879	D_SI1_Lan_0.10_2m_
880	D_SI1_Lan_0.10_3m_
881	D_SI1_Lan_0.10_3m_2P
882	D_SI1_Lan_0.10_3m_2Pa
883	D_SI1_Lan_0.25_3m_2P
884	D_SI1_Lan_0.25_3m_2Pa
885	D_SI1_Lan_0.50_2m_
886	D_SI1_Lan_0.50_3m_
887	D_SI1_Lan_0.75_3m_
888	D_SI1_Lan_0.75_3m_2P
889	D_SI1_Lan_0.75_3m_2Pa
890	D_SI1_Lan_1.00_2m_
891	D_SI1_Lan_1.00_3m_
892	D_SI1_Lan_1.00_3m_2P
893	D_SI1_Lan_1.00_3m_2Pa
894	D_SI1_Lan_1.50_2m_
895	D_SI1_Lan_1.50_3m_
896	D_SI1_Lan_1.50_3m_2P
897	D_SI1_Lan_1.50_3m_2Pa
898	D_SI1_Lan_2.50_2m_
899	D_SI1_Nor_0.02_3m_
900	D_SI1_Nor_0.04_3m_2P
901	D_SI1_Nor_0.04_3m_2Pa
902	D_SI1_Nor_0.10_2m_
903	D_SI1_Nor_0.25_3m_

Number	OpenSees Run Name
904	D_SI1_Nor_0.25_3m_2P
905	D_SI1_Nor_0.25_3m_2Pa
906	D_SI1_Nor_0.50_2m_
907	D_SI1_Nor_0.50_3m_
908	D_SI1_Nor_0.50_3m_2P
909	D_SI1_Nor_0.50_3m_2Pa
910	D_SI1_Nor_1.00_2m_
911	D_SI1_Nor_1.00_3m_
912	D_SI1_Nor_1.00_3m_2P
913	D_SI1_Nor_1.00_3m_2Pa
914	D_SI1_Nor_2.00_2m_
915	D_SI1_Nor_2.00_3m_
916	D_SI1_Nor_2.00_3m_2P
917	D_SI1_Nor_2.00_3m_2Pa
918	D_SI1_Nor_3.00_2m_
919	D_SI1_Nor_4.00_2m_
920	D_SI1_Nor_4.00_3m_
921	D_SI1_Nor_4.00_3m_2P
922	D_SI1_Nor_4.00_3m_2Pa
923	D_SI1_San_0.02_2m_
924	D_SI1_San_0.02_3m_
925	D_SI1_San_0.02_3m_2P
926	D_SI1_San_0.02_3m_2Pa
927	D_SI1_San_0.10_2m_
928	D_SI1_San_0.10_3m_
929	D_SI1_San_0.10_3m_2P
930	D_SI1_San_0.10_3m_2Pa
931	D_SI1_San_0.50_2m_
932	D_SI1_San_0.50_3m_
933	D_SI1_San_0.50_3m_2P
934	D_SI1_San_0.50_3m_2Pa
935	D_SI1_San_1.00_2m_
936	D_SI1_San_1.00_3m_
937	D_SI1_San_1.00_3m_2P
938	D_SI1_San_1.00_3m_2Pa
939	D_SI1_San_1.50_3m_
940	D_SI1_San_1.50_3m_2P
941	D_SI1_San_1.50_3m_2Pa
942	D_SI1_San_2.00_2m_
943	D_SI1_San_2.50_3m_
944	D_SI1_San_2.50_3m_2P
945	D_SI1_San_2.50_3m_2Pa
946	D_SI1_San_4.00_2m

Appendix B

OpenSees Results